Facile Synthesis of Alkynyl− and Vinylidene−Niobocene Complexes. Unexpected η^1-Vinylidene−η^2-Alkyne Isomerization

Cristina García-Yebra,[†] Carmen López-Mardomingo,[†] and Mariano Fajardo[‡]

Departamento de Química Orgánica and Departamento de Química Inorgánica, Campus Universitario, Universidad de Alcalá, 28871 Alcalá de Henares (Madrid), Spain

Antonio Antiñolo, Antonio Otero,* and Ana Rodríguez

Departamento de Química Inorgánica, Orgánica y Bioquímica, Facultad de Química, Universidad de Castilla-La Mancha, 13071 Ciudad Real, Spain

Alain Vallat, Dominique Lucas, and Yves Mugnier

Laboratoire de Synthèse et d'Electrosynthèse Organometalliques associè au CNRS (URA 1685), Faculté des Sciences, 6 Bd. Gabriel, 21000 Dijon, France

Jorge Juan Carbó and Agustí Lledós*

Departament de Química, Universitat Autònoma de Barcelona, 08193 Bellaterra, Barcelona, Spain

Carles Bo

Departament de Química Física i Inorgànica, Universitat Rovira i Virgili, Pl. Imperial Tarraco, 1, 43005 Tarragona, Spain

Treatment of $Nb(\eta^5-C_5H_4SiMe_3)_2(Cl)(L)$ (**1**) with $Mg(C{\equiv}CR)_2$ in toluene, under appropriate reaction conditions, leads to the alkynyl complexes $Nb(\eta^5-C_5H_4SiMe_3)_2(C{\equiv}CR)(L)$ (**2**: L = CO, R = Ph (**2a**); L = CO, R = $SiMe_3$ (**2b**); L = CO, R = ^tBu (**2c**); L = PMe_2Ph, R = Ph (**2d**); L = $P(OEt)_3$, R = Ph (**2e**)). The alkynyl-containing niobocene species **2** can be chemically or electrochemically oxidized to give the corresponding cation-radical alkynyl complexes $[Nb(\eta^5-C_5H_4SiMe_3)_2(C{\equiv}CR)(L)]^{\bullet+}[BPh_4]^-$ (**3**: L = CO, R = Ph (**3a**); L = CO, R = ^tBu (**3c**); L = PMe_2Ph, R = Ph (**3d**)). These complexes, under different experimental conditions, give rise to the mononuclear vinylidene d^2 niobocene species $[Nb(\eta^5-C_5H_4SiMe_3)_2({=}C{=}CHR)(L)][BPh_4]$ (**4**: L = CO, R = Ph (**4a**); L = CO, R = ^tBu (**4c**); L = PMe_2Ph, R = Ph (**4d**)) with a hydrogen atom by abstraction from the solvent or, for **3a**, the binuclear divinylidene d^2 niobocene complex $[(\eta^5-C_5H_4SiMe_3)_2(CO)Nb{=}C{=}C(Ph)(Ph)C{=}C{=}Nb(CO)(\eta^5-C_5H_4SiMe_3)_2][BPh_4]_2$ (**4a′**) from a competitive ligand−ligand coupling process. Complexes **4** were also prepared by an alternative procedure in which the corresponding complexes **2** were reacted with HBF_4. Finally, in solution the CO-containing vinylidene mononuclear complexes **4a** and **4c** undergo an unexpected isomerization process to give the η^2-alkyne derivatives $[Nb(\eta^5-C_5H_4SiMe_3)_2(\eta^2(C,C){-}HC{\equiv}CR)(CO)]^+$ (**5**: R = Ph (**5a**); R = ^tBu (**5c**)). The structure of **5a** was determined by single-crystal diffractometry. DFT calculations were carried out on $[NbCp_2({=}C{=}CHCH_3)(L)]^+/[NbCp_2(HC{\equiv}CCH_3)(L)]^+$ (Cp = $\eta^5-C_5H_5$; L = CO, PH_3; *exo*, *endo*) model systems in order to explain the η^1-vinylidene−η^2-alkyne rearrangement observed. Calculations have shown that in both carbonyl−niobocene and phosphine−niobocene systems the η^1-vinylidene and the η^2-alkyne complexes are isoenergetic, in marked contrast with the systems previously considered in theoretical studies. The reaction takes place through an intraligand 1,2-hydrogen shift mechanism where $\eta^2(C,H)$-alkyne species are involved. The energy barrier for the isomerization process in the phosphine-containing niobocene systems is almost 10 kcal mol^{-1} higher than in the analogous process for the carbonyl-containing niobocene system. This increase in activation barrier indicates that the different experimental behavior between **4a**, **4c,** and **4d** has a kinetic rather than a thermodynamic origin. Finally, the interconversion between *exo* and *endo* isomers has been studied.

Introduction

The chemistry of d-block transition metals with alkynyl,[1] vinylidene,[2] and alkyne[3] ligands has been well-

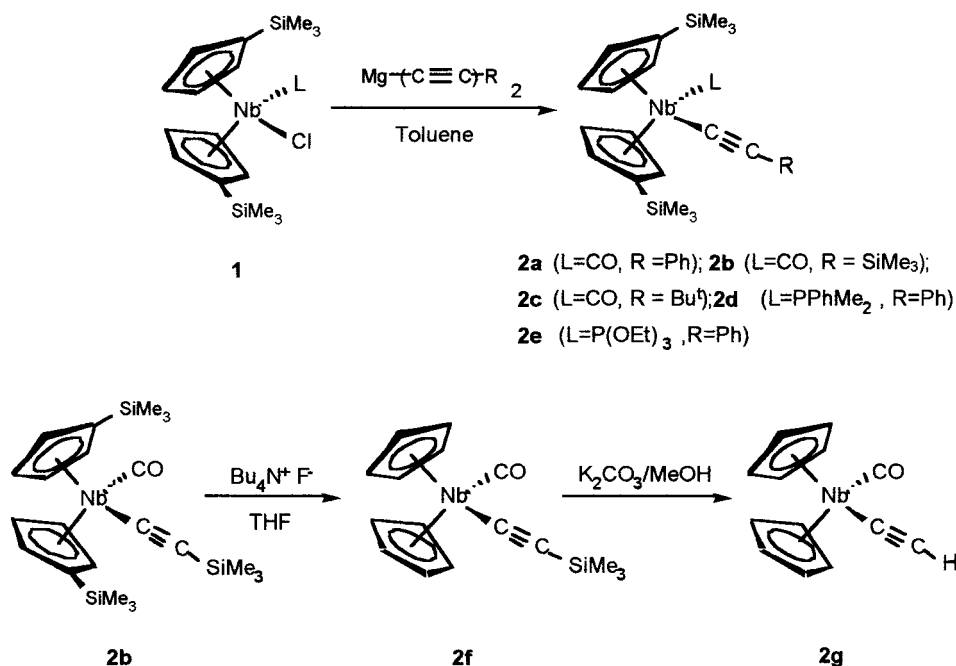documented. During the past few years several families of alkyne-containing halobis(trimethylsilylcyclopen-

---

† Departamento de Química Organica, Universidad de Alcalá.
‡ Departamento de Química Inorganica, Universidad de Alcalá.

(1) (a) Nast, R. *Coord. Chem. Rev.* **1982**, *47*, 89. (b) Bruce, M. I. *Chem. Rev.* **1983**, *83*, 203. (c) Manna, J.; Jonh, K. D.; Hopkins, M. D. *Adv. Organomet. Chem.* **1996**, 79.

Scheme 1

2a (L=CO, R =Ph); **2b** (L=CO, R = SiMe$_3$);
2c (L=CO, R = Bu^t);**2d**   (L=PPhMe$_2$, R=Ph)
2e (L=P(OEt)$_3$,R=Ph)

tadienyl)niobium complexes have been reported by our group,[4] and in particular, several cationic complexes were isolated in good yields as their nitrile or isonitrile adducts, [Nb(η^5-C$_5$H$_4$SiMe$_3$)$_2$(η^2(*C,C*)-RC≡CR′)(L)]$^+$, by one-electron oxidation of the corresponding alkyne-containing niobium(IV) species, Nb(η^5-C$_5$H$_4$SiMe$_3$)$_2$(η^2-(*C,C*)-RC≡CR′).[5] These results encouraged us to explore general synthetic methods for the preparation of alkynyl- and vinylidene-containing niobocene complexes, which are rarely encountered in the literature. The alkynyl and vinylidene species were successfully prepared by reaction of the corresponding haloniobium(III) complexes with the appropriate alkynylmagnesium compounds, Mg(C≡CR)$_2$, followed by one-electron oxidation of the isolated alkynylniobium species and a hydrogen atom abstraction from the solvent. However, surprising behavior was found for some vinylidene–niobocene compounds, which isomerize easily in solution to give the more stable alkyne-containing complexes. The 1-alkyne to vinylidene rearrangement in the coordination sphere of transition metals has proved to be a useful entry to vinylidene complexes,[6] vinylidene apparently being stabilized in many transition-metal complexes, and several catalytic cycles have been proposed involving the participation of the η^1-vinylidene–

η^2-alkyne transformation.[7] Despite the relative importance of this phenomenon, few examples of this type of rearrangement have been described for group 5 elements.[8] This paper will focus on the synthesis and structural characterization of alkynyl-, vinylidene-, and alkyne-containing niobocene complexes and an η^1-vinylidene–η^2-alkyne conversion process. The study of the vinylidene–alkyne rearrangement by means of DFT calculations will also be discussed.

Results and Discussion

Preparation and Characterization of Alkynyl–Niobocene Complexes. The starting niobium complexes Nb(η^5-C$_5$H$_4$SiMe$_3$)$_2$(Cl)(L) (**1**) reacted with the appropriate dialkynylmagnesium reagents, in toluene, to generate the corresponding alkynylniobocene complexes **2** in good yields (Scheme 1). The use of a noncoordinating solvent, such as toluene, has proved to be essential in this process, due to the fact that the reactivity of the magnesium reagent is increased. Attempts to carry out similar reactions with lithium alkynyl reagents or the analogous Grignard alkynyl, MgX(C≡CR), in ethereal solvents have proved unsuccessful. Previous efforts to prepare similar complexes by reacting the halo derivatives M(η^5-C$_5$Me$_5$)$_2$Cl$_2$ (M = Nb, Ta) with LiC≡CR were also unsuccessful.[8] As far as we are aware, this is the first general procedure to prepare σ-alkynyl–niobocene complexes. Tantalum hydrido alkynyl species, Ta(η^5-C$_5$Me$_5$)$_2$(H)(C≡CR), have been proposed as the intermediates in the conversion of η^2-alkyne complexes, Ta(η^5-C$_5$Me$_5$)$_2$(η^2(*C,C*)-HC≡CR), to the corresponding vinylidene species, Ta(η^5-C$_5$Me$_5$)$_2$-

(2) (a) Bruce, M. I.; Swincer, A. G. *Adv. Organomet. Chem.* **1983**, *22*, 59. (b) Bruce, M. I. *Chem. Rev.* **1991**, *91*, 197. (c) Antonova, A. B.; Johansson, A. A. *Russ. Chem. Rev. (Engl. Transl.)* **1989**, *58*, 693.

(3) (a) Ittel, S. D.; Ibers, J. A. *Adv. Organomet. Chem.* **1976**, *14*, 33. (b) Otsuka, S.; Nakamura, A. *Adv. Organomet. Chem.* **1976**, *14*, 245.

(4) (a) Antiñolo, A.; Gómez-Sal, P.; Martínez de Ilarduya, J. M.; Otero, A.; Royo, P.; Martínez-Carrera, S.; García-Blanco, S. *J. Chem. Soc., Dalton Trans.* **1987**, 975. (b) Antiñolo, A.; Fajardo, M.; Jalón, F.; López-Mardomingo, C.; Otero, A.; Sanz-Bernabé, C. *J. Organomet. Chem.* **1989**, *369*, 187. (c) Antiñolo, A.; Fajardo, M.; Gil-Sanz, R.; López-Mardomingo, C.; Otero, A.; Lucas, D.; Chollet, H.; Mugnier, Y. *J. Organomet. Chem.* **1994**, *481*, 27. (d) Antiñolo, A.; Martínez-Ripoll, M.; Mugnier, Y.; Otero, A.; Prashar, S.; Rodríguez, A. M. *Organometallics* **1996**, *15*, 3241.

(5) Antiñolo, A.; Otero, A.; Fajardo, M.; García-Yebra, C.; López-Mardomingo, C.; Martín, A.; Gómez-Sal, P. *Organometallics* **1997**, *16*, 2601.

(6) See for example: Werner, H. *Angew. Chem., Int. Ed. Engl.* **1990**, *29*, 1077.

(7) (a) Landon, S. J.; Shulman, P. M.; Geoffroy, G. L. *J. Am. Chem. Soc.* **1985**, *107*, 6739. (b) Maché, R.; Sasaki, Y.; Bruneau, C.; Dixneuf, P. H. *J. Org. Chem.* **1989**, *54*, 1518. (c) Trost, B. M.; Dyker, G.; Kulawiec, R. J. *J. Am. Chem. Soc.* **1990**, *112*, 7809. (d) Bianchini, C.; Peruzzini, M.; Zanobini, F.; Frediani, P.; Albinati, A. *J. Am. Chem. Soc.* **1991**, *113*, 5453.

(8) Gibson, V. C.; Parkin, G.; Bercaw, J. E. *Organometallics* **1991**, *10*, 220.

Scheme 2
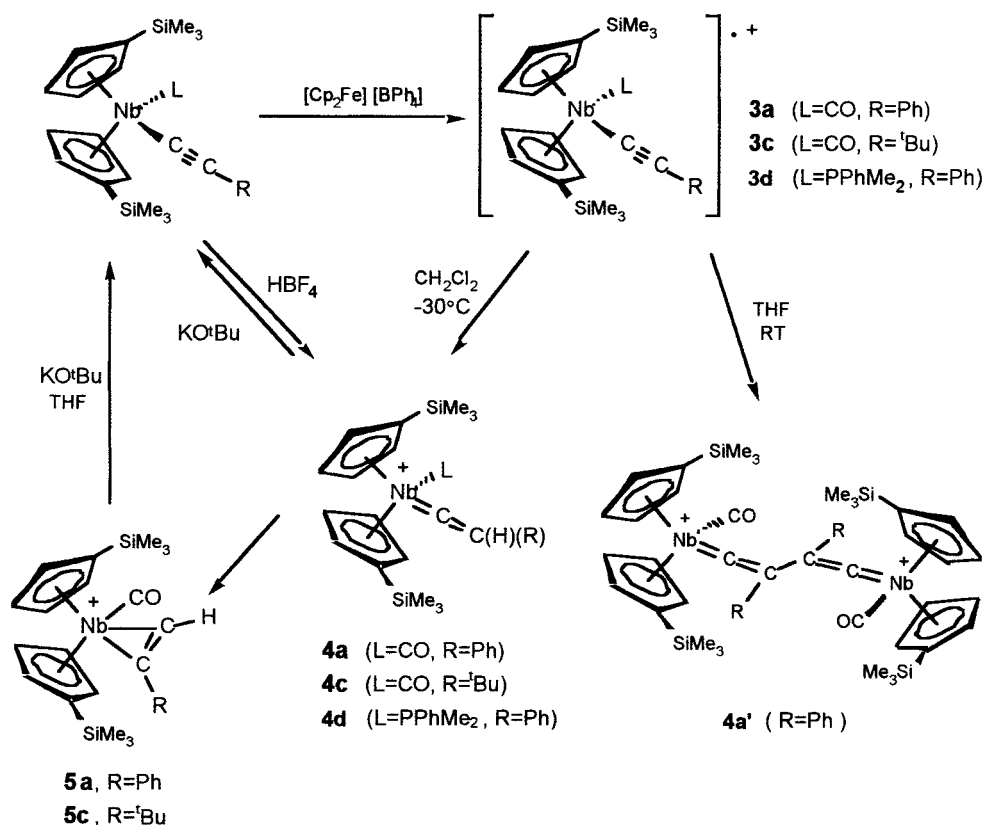
(=C=CH(R)), but such species could not be isolated or identified.[8] Alkynyl-containing cationic tantalocene complexes, $[Ta(\eta^5\text{-}C_5Me_5)_2(NHR')(C\equiv CR)][B(C_6F_5)_4]$, have recently been isolated from carbon–hydrogen bond activation reactions of $[Ta(\eta^5\text{-}C_5Me_5)_2(=NR')(THF)]$-$[B(C_6F_5)_4]$ with propyne or phenylacetylene.[9]

The general procedure described for the preparation of alkynyl–niobocene complexes did not, however, allow the synthesis of terminal alkynyl species (R = H), since the preparation of the reagent $Mg(C\equiv CH)_2$ was not possible. Different lithium reagents, such as $HC\equiv CLi\cdot H_2NCH_2CH_2NH_2$, or Grignard reagents, such as $MgCl$-$(C\equiv CH)$ in THF, were employed as alternatives, but their reactions with **1** under a variety of experimental conditions led to the starting material as the only organometallic product to be isolated from the reaction. To overcome this problem, we sought to desilylate the alkynyl ligand of complex **2b** by reaction with Bu_4NF in THF.[10] However, the complex $Nb(\eta^5\text{-}C_5H_5)_2(C\equiv CSiMe_3)(CO)$ (**2f**), in which the cyclopentadienyl rings had been desilylated, was isolated instead (Scheme 1). A further desilylation of **2f** using K_2CO_3 in methanol[11] was successful, giving the desired terminal alkynyl-containing complex $Nb(\eta^5\text{-}C_5H_5)_2(C\equiv CH)(CO)$ (**2g**) (Scheme 1). Attempts to prepare **2g** by the direct reaction of **2b** with K_2CO_3/CH_3OH were also unsuccessful, and unreacted **2b** (80–90%), contaminated with as yet unidentified products, was isolated. The alkynyl-

containing complexes **2** were characterized by standard spectroscopic methods. The IR spectra of these complexes show a characteristic band at ca. 2000–2100 cm^{-1} ($\nu_{C\equiv C}$) which corresponds to the coordinated alkynyl unit and, in addition, in complexes **2a–c** and **2f,g** one band at 1890–1950 cm^{-1} corresponding to $\nu_{C\equiv O}$. The ^{13}C NMR spectra of these complexes exhibit two characteristic resonances for the alkynyl C_α and C_β carbons near 125 and 103 ppm, respectively. Furthermore, in the carbonyl-containing complexes the resonance of the carbonyl carbon atom appears at ca. 250 ppm (see Experimental Section).

Oxidation Processes of Alkynyl-Containing Niobocene Complexes. Oxidation reactions of complexes **2** have been carried out by chemical and electrochemical methods. First, we considered the chemical oxidation processes of complexes **2** with the ferrocenium salt $[FeCp_2][BPh_4]$ and, in the course of these studies, we observed that the nature of the resulting products depended dramatically on the substituent R on the alkynyl ligand, the ancillary ligand L, and the experimental conditions employed (temperature and solvent). Thus, **2a,c,d** were reacted with the ferrocenium salt in a 1:1 molar ratio, in CH_2Cl_2 at −30 °C, to give the radical cationic alkynyl complexes $[Nb(\eta^5\text{-}C_5H_4SiMe_3)_2$-$(C\equiv CR)(L)]^{\bullet+}[BPh_4]^-$ (**3**) (Scheme 2). The species **3a,c** were unstable, giving rise to the corresponding monovinylidene complexes $[Nb(\eta^5\text{-}C_5H_4SiMe_3)_2(=C=CHR)(L)]$-$[BPh_4]$ (**4**) (Scheme 2), which result from a hydrogen atom abstraction from the solvent. Compound **4a** was isolated as a 1:1 mixture of both *exo* and *endo* isomers and **4c** as a single isomer. To confirm this abstraction process, the oxidation of **2a** was carried out in dry CD_2-Cl_2 at −40 °C and the deuterated complex $[Nb(\eta^5\text{-}C_5H_4$-

(9) Blake, R. E.; Antonelli, D. M.; Henling, L. M.; Schaefer, W. P.; Hardcastle, K. I.; Bercaw, J. E. *Organometallics* **1998**, *17*, 718.

(10) Wong, A.; Kang, P. C. W.; Tagge, C. D.; Leon, D. R. *Organometallics* **1990**, *9*, 1992.

(11) This method was employed to desilylate the complex $[Re(\eta^5\text{-}C_5Me_5)(-C\equiv CC\equiv CSiMe_3)(NO)(PMe_3)]$: Weng, W.; Bartie, T.; Gladysz, J. A. *Angew. Chem., Int. Ed. Engl.* **1994**, *33*, 2199.

SiMe$_3$)$_2$(=C=CDR)(CO)][BPh$_4$] was isolated (established by a ^{2}H NMR spectrum), indicating that in fact the solvent is the source of the H$^{\bullet}$ (or D$^{\bullet}$) radical. Compound **3d**, however, was stable under these experimental conditions and was isolated as a deep red crystalline material after appropriate workup. Solutions of **3d** in CH$_2$Cl$_2$ evolve slowly at room temperature to give, after several weeks, the monovinylidene complex **4d** in low yield. In the case of **2b**, the oxidation process with the ferrocenium salt and the subsequent transformation of the radical cationic alkynyl species in CH$_2$Cl$_2$ gave, in low yield, the unsubstituted monovinylidene complex [Nb(η^5-C$_5$H$_4$SiMe$_3$)$_2$(=C=CH$_2$)(CO)][BPh$_4$] (**4h**), with loss of the SiMe$_3$ group of the alkynyl ligand. Related mononuclear vinylidene tantalocene and niobocene complexes have previously been described.[8,12]

However, when the oxidation of **2a** was carried out in THF solution at room temperature, an alternative product, the divinylidene complex [(η^5-C$_5$H$_4$SiMe$_3$)$_2$(CO)-Nb=C=C(Ph)(Ph)C=C=Nb(CO)(η^5-C$_5$H$_4$SiMe$_3$)$_2$]-[BPh$_4$]$_2$ (**4a′**),[5] was obtained as the major product (Scheme 2), along with a small proportion of the monovinylidene complex **4a**. In THF solution at low temperature, the divinylidene is formed as the minor product. Surprisingly, the formation of the corresponding divinylidene species from compounds **2c,d** has never been observed, even though the oxidation has been attempted under a wide variety of reaction conditions. The formation of the divinylidene species **4a′** can be envisaged as being the result of a ligand–ligand coupling reaction from the radical cationic alkynyl species **3a** instead of the alternative process of hydrogen atom abstraction. The chemistry of 17-electron organometallic radicals is well-documented, and their often characteristic chemical properties continue to be reported.[13] It is well-known that several organometallic radicals tend to dimerize and that dimerization through the metal center is most often observed. Nevertheless, the ligand–ligand coupling could be favored if the metal center is sterically protected and if one of the ligands possesses a π-system to enable the delocalization of the spin density. Thus, Lapinte and co-workers have demonstrated that the iron–ethynyl complex [Fe(η^5-C$_5$Me$_5$)$_2$-(C≡CH)(dppe)] reacts with [FeCp$_2$][PF$_6$] to give a divinylidene complex through a ligand–ligand coupling step.[14] However, they observed that the analogous substituted alkynyl complexes [Fe(η^5-C$_5$Me$_5$)$_2$(C≡CR)-(dppe)] (R = Ph, ^{t}Bu) did not undergo dimerization or hydrogen atom abstraction, and the 17-electron radical cationic alkynyl complexes [Fe(η^5-C$_5$Me$_5$)$_2$(C≡CR)-(dppe)]$^{\bullet+}$[PF$_6$]$^-$ could be isolated as air-stable solids. The low reactivity of these complexes was explained on the basis of the steric hindrance of the substituent attached to the alkynyl carbon atom.[15] In our case, the 17-electron radical species **3a,c** were unstable, and this could be due to the fact that the substituents on the alkynyl group did not provide sufficient steric protection to prevent the transformation to the corresponding vinylidene complexes **4**. This process of hydrogen atom abstraction has been established in the evolution of several organometallic radicals.[16]

In addition, a ligand–ligand coupling reaction to give divinylidene species, versus hydrogen atom abstraction to form monovinylidene species, must be considered as a competitive reaction path in the evolution of the radical alkynyl species, especially in light of the results obtained by reacting complex **2a** in THF under a variety of reaction conditions. It is tempting to speculate that, due to the presence of the more bulky (^{t}Bu) substituent, the radical **3c** cannot undergo the ligand–ligand coupling to give the corresponding divinylidene complex, although electronic factors, such as the capacity of the ligand to delocalize electron density, could play an important role in the reaction of the radical species. However, **3d** was especially stable and electronic factors (the presence of a phosphine instead of a carbonyl as ancillary ligand) and steric factors (a more bulky phosphine as ancillary ligand) could be responsible for this behavior.

Furthermore, complexes **4** could alternatively be prepared by the protonation of complexes **2** with HBF$_4$ (Scheme 2), although the same reaction for **2b** gave an intractable mixture of products that could not be identified. This protonation reaction is reversible, and treatment of **4** with KO^{t}Bu quantitatively gives **2**. The spectroscopic data support the proposed formulations for complexes **3** and **4**. The radical cationic species **3c,d** were spectroscopically characterized by their ESR spectra (see below). The vinylidene α- and β-carbons in **4** exhibit characteristic resonances at ca. 380 and 120 ppm, respectively, in their ^{13}C NMR spectra, which are entirely consistent with the presence of a vinylidene unit.[2b]

Electrochemical Studies. Electrochemical studies on complexes **2a,c,d** have been carried out. The simplest voltammetric profile is obtained for **2d** (Figure 1a and Table 1), which undergoes reversible ($i_{p,O}/i_{p,O'} \approx 1$), diffusion-controlled ($i_{p,O'}/v^{1/2}$ is nearly constant for scan rates varying between 50 and 200 mV s^{-1}) one-electron oxidation to give the corresponding radical cation **3d**. When the controlled-potential electrolysis of **2d** was carried out, at 0 V and -30 °C, it resulted in a coulometric consumption of nearly 1 F mol^{-1} ($n_{exp} = 0.9$). The voltammogram of the electrolyzed solution shows a peak, O (Figure 1), indicating that **3d** was quantitatively generated and was stable on the CV and electrolysis time scale. ESR spectroscopic analysis of this solution confirmed the formation of **3d** as well as its stability (see below). The complex **3d** prepared by chemical oxidation exhibits the same cyclic voltammetric features.

The voltammetric behavior of complexes **2a,c** is more complicated. Thus, the cyclic voltammogram of **2c** at room temperature (see Figure 2a) displays, in addition to the O/O′ system ($i_{p,O}/i_{p,O'} \approx 0.96$), a small peak, R, at lower cathodic potential (see Table 1 for potential values). The latter peak becomes less intense as the sweep rate is made higher, and lowering the temperature to −30 °C results in its complete disappearance (see

(12) (a) Van Asselt, A.; Burger, B. J.; Gibson, V. C.; Bercaw, J. E. *J. Am. Chem. Soc.* **1986**, *108*, 5347. (b) Fermin, M. C.; Bruno, J. W. *J. Am. Chem. Soc.* **1993**, *115*, 7511.

(13) Kuksis, I.; Baird, M. C. *J. Organomet. Chem.* **1997**, *527*, 137 and references therein.

(14) Le Narvor, N.; Toupet, L.; Lapinte, C. *J. Am. Chem. Soc.* **1995**, *117*, 7129.

(15) Connelly, N. G.; Gamasa, M. P.; Gimeno, J.; Lapinte, C.; Lastra, E.; Maher, J. P.; Le Narvor, N.; Rieger, A. L.; Rieger, P. H. *J. Chem. Soc., Dalton Trans.* **1993**, 2575.

(16) See, for example: Iyer, R. S.; Selegue, J. P. *J. Am. Chem. Soc.* **1987**, *109*, 910.
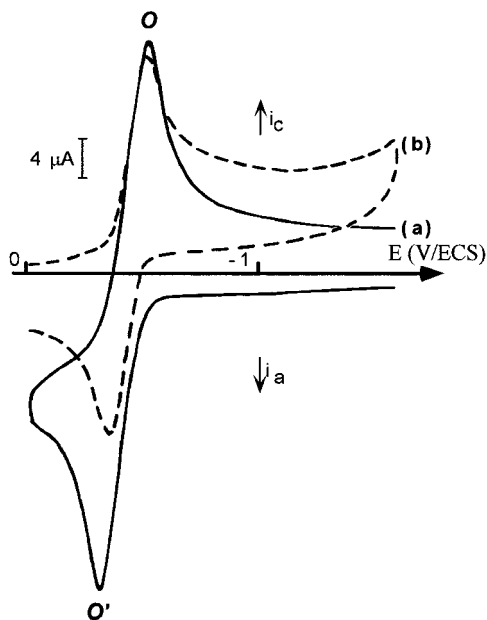
Figure 1. Cyclic voltammograms of **2d** (3.5 mM) in THF/ 0.2 M NBu$_4$ClO$_4$ on a vitreous carbon disk electrode: (a) before electrolysis at room temperature; (b) after electrolysis at 0 V at −30 °C. Scan rate: 200 mV s^{-1}. Initial potential: −1.6 V (a) and 0 V (b).

Table 1. Cyclic Voltammetric Data^a for the Complexes Nb(η^5-C$_5$H$_4$SiMe$_3$)$_2$(L)(C≡CR)

compd	L	R	$E_{1/2,O'}{}^b$ (V/ECS)	$E_{p,R}$ (V/ECS)
2a	CO	Ph	+0.27	−0.91
2c	CO	^{t}Bu	+0.20	−1.04
2d	PMe$_2$Ph	Ph	−0.43	

^{a} In THF/0.2 M NBu$_4$PF$_6$ on vitreous carbon disk electrode at a scan speed of 200 mV s^{-1}. ^{b} Taken as the half-sum of $E_{p,O'}$ and $E_{p,O}$.[17]

Figure 2b), as $i_{p,O}/i_{p,O'}$ becomes nearly equal to 1. These changes are strongly indicative of an EC-type mechanism where the corresponding electrogenerated cation radical alkynyl species **3c** undergoes a chemical evolution.

With the aim of stabilizing **3c**, an exhaustive electrolysis was performed at −30 °C in THF with NBu$_4$-ClO$_4$ as the supporting electrolyte. Complex **3c** consumes nearly 1 equiv of electron (working electrode potential, +0.4 V vs ECS; n_{exp} = 0.95), and the cyclic voltammogram of the electrolyzed solution (still registered at low temperature) does show peak O to some extent but mainly consists of peak R (see Figure 2c) together with small ill-defined peaks that appear in the range 0−1 V. The ESR spectrum of this electrolyzed solution indicates the presence of **3c** (see below). When the temperature is raised to room temperature, peak O disappears (see Figure 2d) and, at the same time, the solution becomes ESR silent. An electrochemical study of complex **2a** gives similar results: oxidation leads to a diamagnetic complex through the transient cation radical alkynyl **3a**. This last product can be reduced near −1 V (see Table 1). However, a question remains: what is the nature of the final diamagnetic products that are reduced at peak R? The chemical oxidation experiments have proven that, starting from the radical cationic alkynyl complexes **3**, there are two reaction pathways: either ligand−ligand coupling, to give the

divinylidene species, or solvent-based hydrogen transfer, giving rise to monovinylidene compounds. To determine which mechanism operates in the course of the electro-chemical oxidation, kinetic information has been extracted from the change in the voltammetric profile with the concentration of **2a**. Figure 3a displays the cyclic voltammogram of **2a** in THF at room temperature at c = 0.8 mM, and the only reduction peak O is observed on the reverse sweep. In contrast, when the concentration is raised to a much higher value (c = 3.7 mM), then peak R appears (Figure 3b). This result is in accordance with the dimerization pathway (a bimolecular reaction following second-order kinetics).[18a] Concentration has no effect on the relative peak intensities (R versus O) in an EC-type mechanism if the associated chemical reaction kinetic is first order,[18b] as is the case in the pathway involving hydrogen atom abstraction. As definitive proof, we measured the cyclic voltammogram of a chemically prepared sample of the divinylidene **4a′**, which exhibits the expected peak R. However, we also confirmed that the cyclic voltammogram of a chemically prepared sample of **4c** exhibits the peak R, indicating, as was previously mentioned for the chemical oxidation of **2c**, that the cation radical alkynyl species **3c** evolves exclusively to give **4c** by hydrogen atom abstraction from the solvent.

Complexes **3c,d** were characterized by ESR spectroscopy. Isotropic g and splitting constant values are listed in Table 2. The spectrum of **3c** exhibits a characteristic 10-line shape arising from coupling between the unpaired spin and the niobium nucleus (100% natural abundance, $I = {}^9/_2$). In the case of **3d**, the spectrum (see Figure 4) consists of a decet of doublets due to additional superhyperfine coupling with phosphorus (a_P = 22.07 G). This last value compares quite well with that found for the analogous chloro complex [Nb(η^5-C$_5$H$_4$SiMe$_3$)$_2$-(Cl)(P(OMe)$_3$)]$^+$ (a_P = 21.85 G).[19] The outer lines are poorly resolved relative to the inner lines due to a considerable increase in line width at the ends of the spectrum, a trend that has been well-established for this type of radical.[20] More informative are the values of the isotropic hyperfine splitting constant, which are nearly identical for both complexes (**3c**, a_{Nb} = 67.88 G; **3d**, a_{Nb} = 70.97 G). This similarity reflects the degree of metal character of the singly occupied molecular orbital. Typical niobocene derivatives NbCp$_2$X$_2$ (X = alkyl, halogeno) exhibit values that lie in the range 80−120 G,[21] whereas complexes with σ-donor−π-acceptor ligands in the equatorial plane NbCp$_2$(L) (L = ketenimine,[22] ketene,[23] acetylene,[24] aldehyde[25]) exhibit smaller a_{Nb} values (8−20 G) due to appreciable delocalization of the

(17) Noel, M.; Vasu, K. I. *Cyclic Voltammetry and the Frontiers of Electrochemistry*; Aspect Publications: London, 1990.
(18) (a) Olmstead, M. L.; Hamilton, R. G.; Nicholson, R. S. *Anal. Chem.* **1969**, *41*, 260. (b) Nicholson, R. S.; Shain, I. *Anal. Chem.* **1964**, *36*, 706.
(19) Lucas, D.; Mugnier, Y.; Antiñolo, A.; Otero, A.; Fajardo, M. *J. Organomet. Chem.* **1992**, *435*, C3−C7.
(20) Savaranamuthu, A.; Bruce, A. E.; Bruce, M. R. M.; Fermin, M. C.; Hneihen, A. S.; Bruno, J. W. *Organometallics* **1992**, *11*, 2190 and references therein.
(21) (a) Manzer, L. E. *Inorg. Chem.* **1977**, *16*, 525. (b) Broussier, R.; Normand, F.; Gautheron, B. *J. Organomet. Chem.* **1978**, *155*, 337. (c) Al-Mowali, A.; Kuder, W. A. A. *J. Organomet. Chem.* **1978**, *155*, 337. (d) Hitchcock, P. B.; Lappert, M. F.; Milne, C. R. C. *J. Chem. Soc., Dalton Trans.* **1981**, 180. (e) Bottomley, F.; Keizer, P. N.; White, P. S.; Preston, K. F. *Organometallics* **1990**, *9*, 1916. (f) Brunner, H.; Gehart, G.; Meier, W.; Wachter, J.; Riedel, A.; Elkrami, S.; Mugnier, Y.; Nuber, B. *Organometallics* **1994**, *13*, 134.
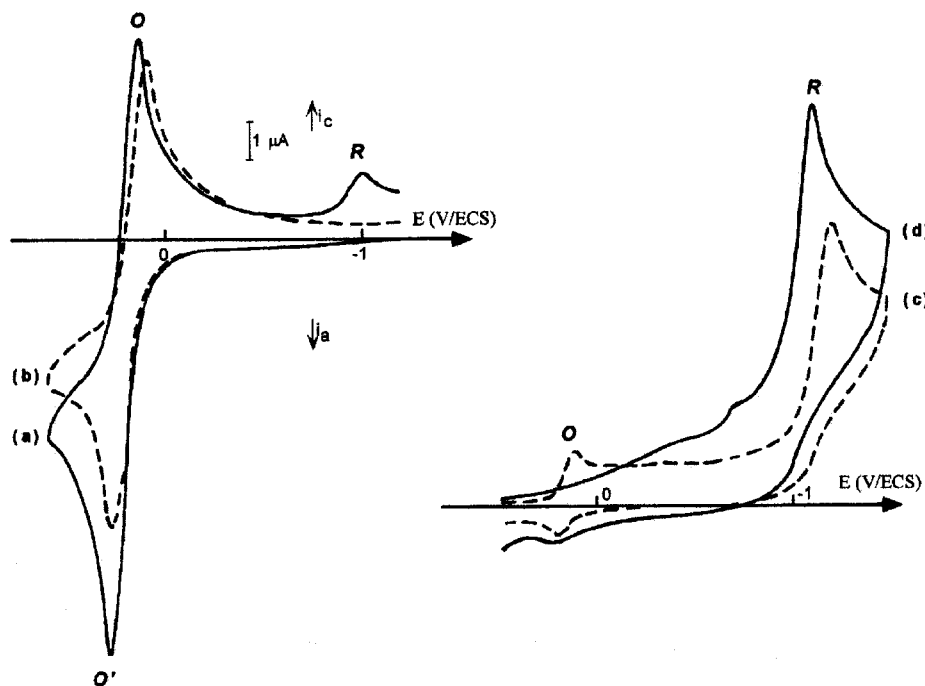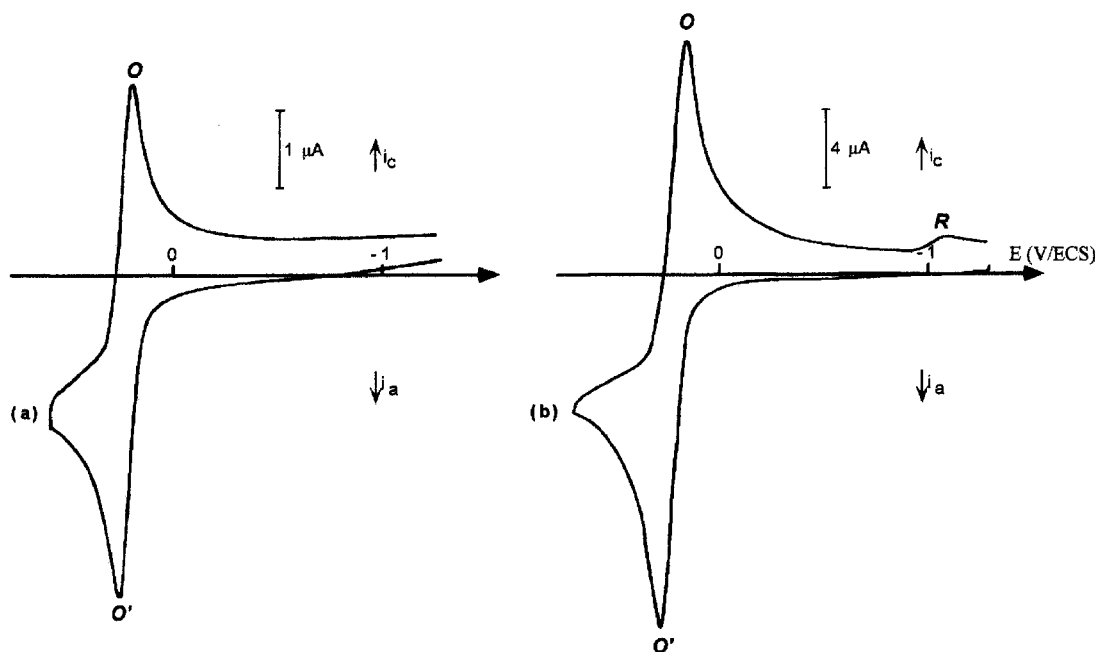
Figure 2. Cyclic voltammograms of **2c**.

Figure 3. Cyclic voltammograms of **2a**.

**Table 2. ESR Data^a for the Complexes
[Nb(η^5-C$_5$H$_4$SiMe$_3$)$_2$(L)(C≡CR)]$^+$**

compd	g	a_{Nb} (G)	a_P (G)
3c	1.9979	67.88	
3d	1.9966	70.97	22.07

^{a} Hyperfine coupling constants and isotropic *g* factors are all corrected to second order using the Breit−Rabi equation.

unpaired electron onto the organic ligand, as has been demonstrated by theoretical calculations.[26] The a_{Nb} values found for **3c,d** are intermediate between the two sets of a_{Nb} values described above and denote a partial

localization of the unpaired spin density on the alkynyl ligand.

Isomerization of η^1-Vinylidene− to η^2-Alkyne−Niobocene Complexes. Although stable in the solid state, the aforementioned vinylidene complexes **4a,c** undergo a rearrangement in THF or acetonitrile solu-

(22) Antiñolo, A.; Fajardo, M.; Lopez-Mardomingo, C.; Otero, A.; Mourad, Y.; Mugnier, Y.; Sanz-Aparicio, J.; Fonseca, I.; Florencio, F. *Organometallics* **1990**, *9*, 2919.

(23) (a) Halfon, S. E.; Fermin, M. C.; Bruno, J. W. *J. Am. Chem. Soc.* **1989**, *111*, 8738. (b) Antiñolo, A.; Fajardo, M.; Lopez-Mardomingo, C.; Otero, A.; Lucas, D.; Mugnier, Y.; Lanfranchi, M.; Pellinghelli, M. A. *J. Organomet. Chem.* **1992**, *435*, 55.

(24) Antiñolo, A.; Fajardo, M.; Lopez-Mardomingo, C.; Otero, A.; Lucas, D.; Mugnier, Y.; Galakhov, M.; Gil-Sanz, R.; Chollet, H. *J. Organomet. Chem.* **1994**, *481*, 27.

(25) Antiñolo, A.; Fajardo, M.; Otero, A.; Lucas, D.; Mugnier, Y.; Chollet, H. *J. Organomet. Chem.* **1992**, *426*, C4.

(26) Antiñolo, A.; Fajardo, M.; Otero, A.; De Jesus, E.; Mugnier, Y. *J. Organomet. Chem.* **1994**, *470*, 127.
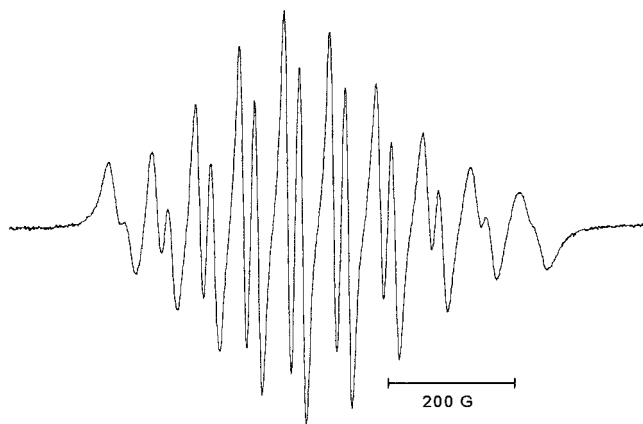
Figure 4. ESR spectrum (X band) of **3d** (solvent: THF, room temperature).

Table 3. Selected Bond Lengths and Angles for Complex 5a

Distances (Å)			
Nb(1)−C(5)	2.094(7)	Nb(1)−C(102)	2.082(6)
Nb(1)−C(7)	2.222(5)	O(4)−C(5)	1.120(7)
Nb(1)−C(6)	2.278(6)	C(6)−C(7)	1.219(7)
Nb(1)−C(101)	2.0856(7	C(7)−C(8)	1.467(7)
Angles (deg)			
C(5)−Nb(1)-C(7)	102.6(2)	C(6)−C(7)−C(8)	146.2(6)
C(5)−Nb(1)−C(6)	71.3(2)	O(4)−C(5)−Nb(1)	178.7(6)
C(7)−Nb(1)−C(6)	31.4(2)	Nb(1)−C(7)−C(8)	137.0(4)

tions at room temperature to give, quantitatively, the more stable η^2-alkyne complexes [Nb(η^5-C$_5$H$_4$SiMe$_3$)$_2$-(η^2(*C,C*)-HC≡CR)(CO)]$^+$ (**5**) (Scheme 2). Thus, the mixture of *endo* and *exo* isomers of **4a** gave the η^2-alkyne-containing complex **5a**, isolated as the pure *exo* isomer. Similar treatment of **4c** led to a 1:1 mixture of isomers of **5c**. In contrast with this behavior, solutions of **4d** were stable even when a CD$_3$CN solution in a sealed NMR tube was heated to 180 °C. Particularly diagnostic of the coordinated alkyne unit in complexes **5** is the presence of a characteristic $\nu_{C≡C}$ band in the IR spectra (ca. 1772 cm^{-1}) and resonances for the nonequivalent carbon atoms in the ^{13}C NMR spectra (ca. 111 and 132 ppm), which are in agreement with the previously reported data for alkyne-containing cationic niobocene complexes.[5] The crystal structure of **5a** consists of an organometallic cation and a BF$_4^-$ anion without any particular cation−anion interaction. Selected bond lengths and angles are depicted in Table 3. The molecular structure of the cation represents a wedgelike sandwich with an angle of 45.7° between the near-planar cyclopentadienyl rings. The relative orientation of the Cp′ rings is intermediate between eclipsed and staggered, as indicated by the Si−C101−C102−Si3 angle of 88° (C(101) and C(102) are the centroids of the Cp′ rings).

Figure 5 clearly indicates the *exo* geometry for alkyne coordination with respect to the carbonyl ligand; the phenyl group of the alkyne is located in the *exo* position to release the steric interaction Nb−CO. The Nb(1)−C(6) distance (2.278(6) Å) is slightly longer than the Nb-(1)−C(7) length (2.222(5) Å). The C(6), C(7), and C(5) atoms are coplanar with the Nb atom, a situation that is in accord with general structural features of penta-coordinated niobocene derivatives. Finally, treatment of **5a,c** with KO^{t}Bu in THF solution allowed us to
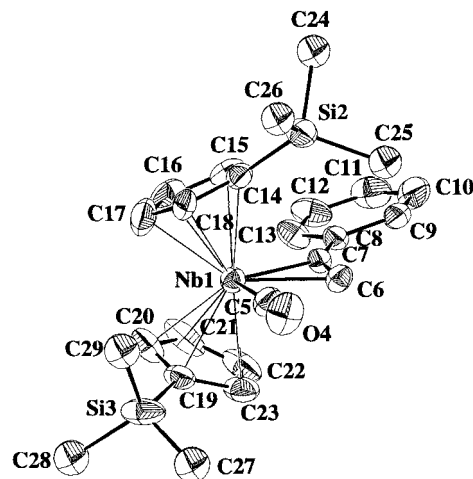

Figure 5. ORTEP drawing of complex **5a**.

recover quantitatively the corresponding η^1-alkynyl complexes **2a,c**, respectively (Scheme 2). Although η^1-vinylidene−η^2-alkyne isomerizations are rare, a few examples have recently been described.[27] In an elegant and exhaustive work, Bly and co-workers[27c] have explained the isomerization of complexes [Cp(CO)$_2$Fe=C=CR^{1}R^2]$^+$OTf$^-$ to the corresponding η^2-alkyne derivatives [Cp(CO)$_2$Fe(η^2-R^{1}C≡CR^2)]$^+$OTf$^-$, through a 1,2-shift of an alkyl group from the β-carbon to the α-carbon, favored by both the extreme electrophilicity of the vinylidene α-carbon and the high π-acidity of the auxiliary carbonyl ligand, which gives rise to an electron-deficient metal center. In the same way, Connelly and co-workers[27a,d,g] have extensively studied the η^1-vinylidene−η^2-alkyne isomerization induced by one-electron oxidation of the 18-electron complexes [(η^6-C$_6$R$_6$)(CO)$_2$Cr=C=CR^{1}R^2]$^+$. The facile isomerization process observed for complexes **4a,c** could be explained on the basis of analogous arguments. Thus, the presence of a strong π-acid carbonyl ligand in the cationic d^2 Nb-(III) species **4a,c** would explain the higher electrophilicity of the vinylidene α-carbon (^{13}C NMR spectroscopic data indicate that this carbon atom in **4a** is more deshielded than that in **4d**, ca. 378 ppm vs 368 ppm, respectively) in these complexes in comparison with the behavior of the α-carbon in complex **4d**, and consequently, the aforementioned η^1-vinylidene−η^2-alkyne rearrangement would be especially favored. This aspect will be analyzed in the next section by means of theoretical calculations.

Theoretical Study. Relative Stability of the Vinylidene and Acetylene Isomers. The first point to be addressed in the theoretical study was the relative stabilities of the η^1-vinylidene and η^2-alkyne complexes. The geometries of the *exo* (**x**) and *endo* (**n**) isomers of the model complexes [NbCp$_2$(=C=CH(CH$_3$))(L)]$^+$ (L = CO, **4^{CO}**; L = PH$_3$, **4^{PH_3}**) and [NbCp$_2$(η^2(*C,C*)-HC≡

(27) (a) Connelly, N. G.; Orpen, G.; Rieger, A. L.; Rieger, P. H.; Scott, C. J.; Rosair, G. M. *J. Chem. Soc., Chem. Commun.* **1992**, 1293. (b) Bly, R. S.; Raja, M.; Bly, R. K. *Organometallics* **1992**, *11*, 1220. (c) Bly, R. S.; Zhong, Z.; Kane, C.; Bly, R. K. *Organometallics* **1994**, *13*, 889. (d) Connelly, N. G.; Geiger, W. E.; Lagunas, M. C.; Metz, R.; Rieger, A. L.; Rieger, P. H.; Shaw, M. J. *J. Am. Chem. Soc.* **1995**, *117*, 12202. (e) Nombel, P.; Lugan, N.; Mathieu, R. *J. Organomet. Chem.* **1995**, *503*, C22. (f) Gamasa, M. P.; Gimeno, J.; González-Bernardo, C.; Borge, J.; García-Granda, S. *Organometallics* **1997**, *16*, 2483. (g) Bartlett, I. M.; Connelly, N. G.; Martin, A. J.; Orpen, A. G.; Paget, T. J.; Rieger, A. L. *J. Chem. Soc., Dalton Trans.* **1999**, 691.
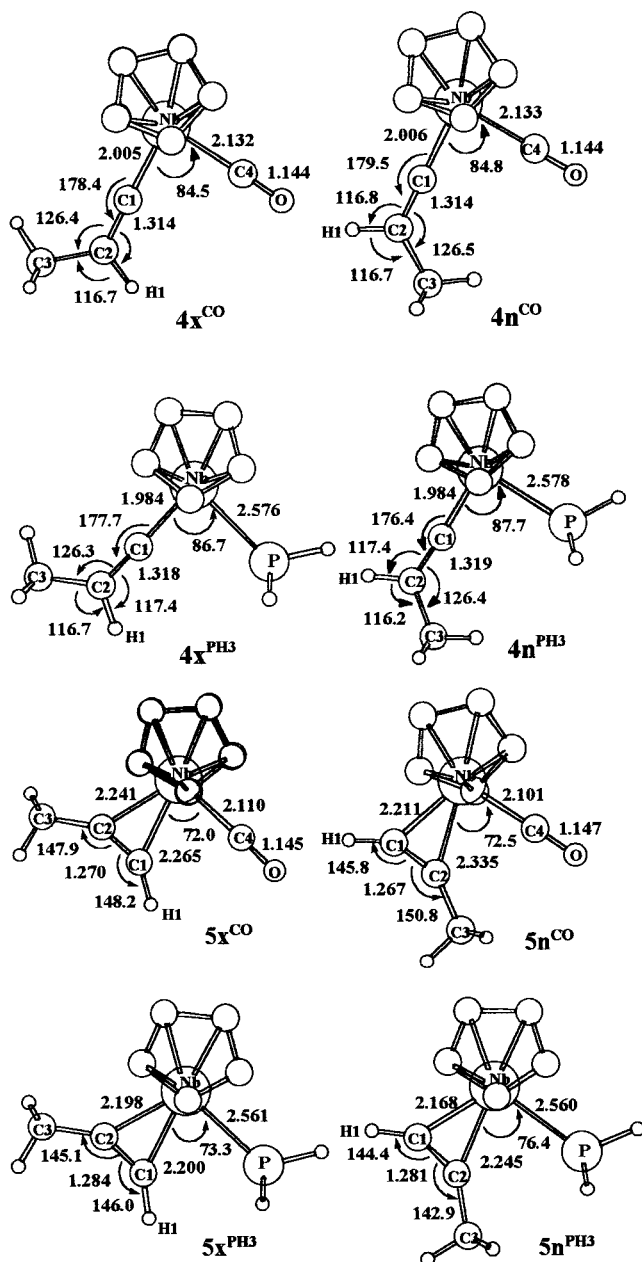
Figure 6. Optimized B3LYP structures (Å, deg) of reactants and products for isomerization of [NbCp$_2$(=C=CHCH$_3$)(L)]$^+$ to [NbCp$_2$(HC≡CCH$_3$)(L)]$^+$. Hydrogen atoms of Cp rings are omitted for simplicity.

CCH$_3$)(L)]$^+$ (L = CO, **5**^{CO}; L = PH$_3$, **5**^{PH_3}) were fully optimized under the constraints of the C_s symmetry group (Figure 6). For comparative purposes we also considered the *exo* η^1-vinylidene and η^2-alkyne niobocenes with L = Cl (**4x**^{Cl} and **5x**^{Cl}, respectively). The calculated Nb–Cl, C≡C, and Nb–C distances in **5x**^{Cl} (2.565, 1.288, and 2.135 and 2.178 Å, respectively) agree well with the distances determined by X-ray diffraction in Nb(η^5-C$_5$H$_4$SiMe$_3$)$_2$(η^2(*C,C*)-PhC≡CPh)Cl (2.538(2), 1.27(1), and 2.185(9) and 2.171(8) Å, respectively).[4a]

In all cases the *exo* isomer appears as the most stable one, but the energy difference between the *exo* and *endo* isomers of all complexes is very small. The calculated energy differences for the vinylidene and alkyne complexes with L = CO and the vinylidene complex with L = PH$_3$ are less than 0.1 kcal/mol. A more marked

destabilization (1.7 kcal/mol) of the *endo* form of **5**^{PH_3} is found, showing that the alkyne isomers are more influenced by steric effects than the corresponding vinylidene analogues. The alkyne substituent preferentially occupies the outside site. It can be expected that energy differences found in model systems increase in real systems, due to the steric effects caused by the presence of bulkier substituents in alkyne and phosphine ligands. In the following discussion we will compare the energies of the *exo* isomers.

The most striking result of the thermodynamic study is the very similar energies of the vinylidene- and alkyne-containing niobocenes. **4x**^{CO}, **4x**^{PH_3}, and **4x**^{Cl} are calculated to be only 0.8, 1.3, and 1.4 kcal/mol more stable than their respective η^2-alkyne-containing niobocene isomers. This is in marked contrast with the systems previously considered in theoretical studies.[28] The effect of ligand substitution on the relative stabilities seems minor, although it always appears that replacement of a strong π-acid CO ligand by a less π-acid PH$_3$ ligand favors the vinylidene form. The energetic results suggest that both the vinylidene– and alkyne–niobocene complexes could be prepared experimentally. The energy differences between the two forms that were found are within the limits of accuracy of the modeling and the methodology employed, but a definitive answer with regard to which is the most stable species cannot be established. We described in the preceding section that **4a,c** isomerize to the corresponding η^2-alkyne-containing species **5a,c**. However, when CO is replaced by a phosphine ligand in **4d**, the analogous isomerization process does not take place. This fact has been related to the higher electrophilicity of the vinylidene α-carbon (C$_\alpha$) in cationic complexes with CO ligands.[27c] Computed NBO charges for the α-carbon are −0.12e in **4x**^{Cl}, −0.08e in **4x**^{PH_3}, and −0.03 in **4x**^{CO}. In agreement with the ^{13}C NMR data, the replacement of CO by PH$_3$ causes an increase in the electron density at the α-carbon. In line with previous arguments,[27c] the thermodynamics of the η^1-vinylidene−η^2-alkyne isomerization in niobocene complexes follows the same trend as the vinylidene C$_\alpha$ charges; therefore, the relative stability of η^1-vinylidene decreases as the electron density at C$_\alpha$ diminishes. However, small differences in the relative energies found do not seem to justify the opposite experimental behavior exhibited by **4a,c** and **4d**. To account for this phenomenon, we will focus in the next section on the kinetics of the isomerization.

Mechanism of the η^1-Vinylidene−η^2-Alkyne Isomerization. Two intramolecular mechanisms are well-documented in the literature for the η^2-alkyne → η^1-vinylidene rearrangement in the coordination sphere of transition-metal complexes: the 1,2-hydrogen shift and the 1,3-hydrogen shift.[2] We considered these two intramolecular mechanisms for the isomerization of the η^1-vinylidene complexes [NbCp$_2$(η^1-CCHCH$_3$)(L)]$^+$ (L = CO, PH$_3$) to the corresponding η^2-alkyne derivatives. Starting from the vinylidene species, in the first mechanism a 1,2-hydrogen shift from the β- to α-carbon takes place, followed by a slippage process of the alkyne ligand from a σ η^2(*C,H*) coordination to a π η^2(*C,C*) coordina-

(28) (a) Wakatsuki, Y.; Koga, N.; Yamazaki, H.; Morokuma, K. *J. Am. Chem. Soc.* **1994**, *116*, 8105. (b) Wakatsuki, Y.; Koga, N.; Werener, H.; Morokuma, K. *J. Am. Chem. Soc.* **1997**, *119*, 360. (c) Stegmann, R.; Frenking, G. *Organometallics* **1998**, *17*, 2089.

tion. Early qualitative theoretical studies[29] supported this mechanism. MP2 calculations have proved that the alkyne−vinylidene rearrangement in the $RuX_2(PR_3)_2 + HC\equiv CHR'$ systems takes place with this mechanism.[28a] The second mechanism consists of the 1,3-hydrogen shift from the β-carbon to the metal, giving rise to an (alkynyl)hydridometal intermediate that undergoes a reductive elimination to form the alkyne-containing species. There is also experimental evidence to suggest that isomerization can proceed via an (alkynyl)hydridometal intermediate.[30−33] Recent theoretical work has shown that the η^2-alkyne → η^1-vinylidene rearrangement in [RhCl(PH$_3$)$_2$(HCCH)] takes place by an intermolecular process via the hydrido intermediate [RhHCl-(PH$_3$)$_2$(CCH)].[28b] Our study is concerned with the intramolecular mechanisms, because steric repulsions caused by the Cp-substituted rings may work against an intermolecular mechanism in the niobocene systems considered here.

We have explored the reaction path for both *exo* and *endo* isomers. Possible intermediates (Figure 7) and transition states (Figure 8) associated with each mechanism were located and the activation barriers determined (Figures 9 and 10).

(i) Reaction Intermediates. For the isomerization of **4**^{CO} and **4**^{PH_3} two kinds of intermediates have been found in the potential energy surfaces: hydrido alkynyl species **A**, which are related to the 1,3-hydrogen shift mechanism, and $\eta^2(C,H)$ alkyne complexes **B**, which are involved in the 1,2-hydrogen shift mechanism.

For the niobocene system with a carbonyl ligand we located two hydrido alkynyl minima (**Ax**^{CO} and **An**^{CO}; see Figure 7). In **Ax**^{CO} the hydrido is cis to the carbonyl ligand, whereas in **An**^{CO} the alkynyl is cis to the carbonyl ligand. Both hydrido alkynyl complexes are very destabilized with respect to the reactant. **Ax**^{CO} and **An**^{CO} are found 38.3 and 32.3 kcal/mol above the vinylidene complexes **4x**^{CO} and **4n**^{CO}, respectively. Two similar minima have been found in the niobocene system with the phosphine ligand (**Ax**^{PH_3} and **An**^{PH_3}). The *cis* hydrido phosphine **Ax**^{PH_3} and the *cis* alkynyl phosphine **An**^{PH_3} isomers lie 38.2 and 25.6 kcal/mol above **4x**^{PH_3} and **4n**^{PH_3}, respectively. The highest stability of the hydrido alkynyl complex with the hydrido in a lateral site could be related to a stronger Nb−H bond for this disposition of the ligands. The Nb−H distance is notably shorter in the **An** isomers than in the **Ax** ones.

The four $\eta^2(C,H)$-alkyne-containing reaction intermediates [NbCp$_2$(L)($\eta^2(C,H)$-(HCCCH$_3$)]$^+$ (L = CO, *exo* (**Bx**^{CO}) and *endo* (**Bn**^{CO}); L = PH$_3$, *exo* (**Bx**^{PH_3}) and *endo* (**Bn**^{PH_3}); see Figure 7) were located in the potential

(29) Silvestre, J.; Hoffmann, R. *Helv. Chim. Acta* **1985**, *65*, 1461.

(30) (a) Nesmeyanov, A. N.; Aleksandrov, G. G.; Antonova, A. B.; Anisimov, K. N.; Kolobova, N. E.; Struchkov, Yu.-T. *J. Organomet. Chem.* **1976**, *110*, C36. (b) Antonova, A. B.; Kolobova, N. E.; Petrovsky, P. V.; Lokshin, B. V.; Obeyzuk, N. S. *J. Organomet. Chem.* **1977**, *137*, 55.

(31) (a) Wolf, J.; Werner, H.; Serhadli, O.; Ziegler, M. L. *Angew. Chem., Int. Ed. Engl.* **1983**, *22*, 414. (b) Garcia Alonso, F. J.; Hoehn, A.; Wolf, J.; Otto, H.; Werener, H. *Angew. Chem., Int. Ed. Engl.* **1985**, *24*, 406. (c) Werner, H.; Garcia Alonso, F. J.; Otto, H.; Wolf, J. *Z. Naturforsch.* **1988**, *43B*, 722. (d) Dziallas, M.; Werener, H. *J. Chem. Soc., Chem. Commun.* **1987**, 852.

(32) Bianchini, C.; Peruzzini, M.; Vacca, A.; Zanobini, F. *Organometallics* **1991**, *10*, 3697.

(33) De los Rios, I.; Jiménez-Tenorio, M.; Puerta, M. C.; Valerga, P. *J. Am. Chem. Soc.* **1997**, *119*, 6529.

Figure 7. Optimized B3LYP structures (Å, deg) of intermediates for isomerization of [NbCp$_2$(=C=CHCH$_3$)(L)]$^+$ to [NbCp$_2$(HC≡CCH$_3$)(L)]$^+$. Hydrogen atoms of Cp rings are omitted for simplicity.

energy surfaces. They are situated between 20 and 30 kcal/mol above their corresponding vinylidene forms. The lengthening of the C−H distances with respect to their values in the $\eta^2(C,C)$-alkyne complexes, as well as the distortion of the C−C−H angle to values between 132.5 and 138.2°, are in accordance with the $\eta^2(C,H)$ nature of these species and indicate that an interaction of the C−H bond with the metal center contributes to the stabilization of the σ-alkyne intermediates. σ η^2-(C,H)-alkyne complexes similar to those presented here have also been found in theoretical studies of the 1,2-

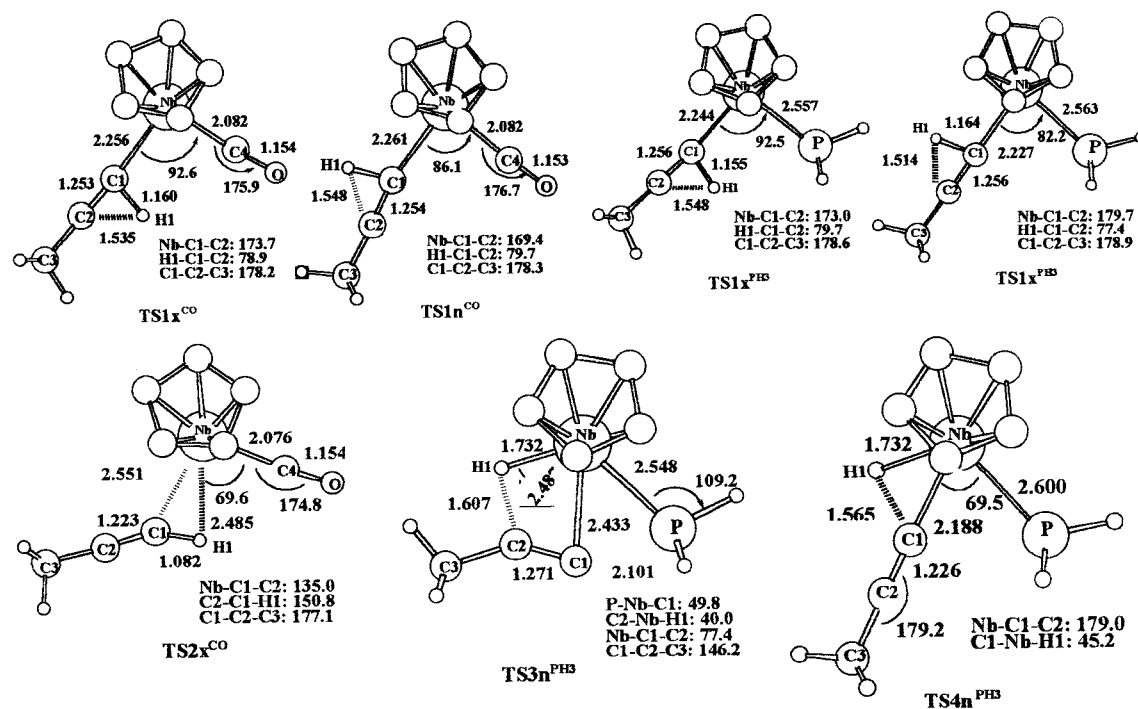**Figure 8.** Optimized B3LYP structures (Å, deg) of transition states for isomerization of $[NbCp_2(=C=CHCH_3)(L)]^+$ to $[NbCp_2(HC≡CCH_3)(L)]^+$. Hydrogen atoms of Cp rings are omitted for simplicity.

mechanism for the alkyne → vinylidene rearrangement.[28,34] The existence of the metal–CH interaction was confirmed by a Bader analysis[35] of the electron density of Bn^{PH_3}. Two bond critical points, one between Nb and H and the other between Nb and C and a ring critical point between Nb, C, and H, were found.

In the niobocene carbonyl system the *exo* and *endo* $η^2(C,H)$-alkyne-containing intermediates display similar energies. Bx^{CO} and Bn^{CO} are found 21.1 and 22.2 kcal/mol above the vinylidene-containing compounds $4x^{CO}$ and $4n^{CO}$, respectively. Both are manifestly more stable than the hydrido alkynyl complexes Ax^{CO} and An^{CO}, respectively. In the niobocene phosphine systems, the intermediates Bx^{PH_3} and Bn^{PH_3} are situated 28.5 and 23.9 kcal/mol above the corresponding vinylidene complexes $4x^{PH_3}$ and $4n^{PH_3}$, respectively. When a phosphine is present as an ancillary ligand, the *endo* $η^2(C,H)$-alkyne Bn^{PH_3} and *endo* hydrido alkynyl An^{PH_3} intermediates become very close in energy. Bn^{PH_3} is found only 1.7 kcal/mol below the hydrido alkynyl An^{PH_3}.

(ii) Reaction Path for the $η^1$-Vinylidene → $η^2$-Alkyne Isomerization. During the course of this study we looked for the transition states that connect the different minima. For the niobocene system with the carbonyl ligand, a transition state for the 4^{CO} → B^{CO} transformation was found for each isomer (*exo* and *endo*). These transition structures ($TS1x^{CO}$ and $TS1n^{CO}$) correspond to the 1,2-hydrogen shift from the vinylidene $C_β$ to the $C_α$. Their geometries (Figure 8) are similar to those theoretically determined for the 1,2-mechanism in the rearrangement $η^2(C,H)$-alkyne → vinylidene in Ru(II)[28a] and Os(II)[34] metallic systems. In both systems a transition state with a planar arrangement of the

C_2H_2 moiety was found. Recently, Stegmann and Frenking have characterized a nonplanar transition state structure for the 1,2-rearrangement on the coordination sphere of the F_4W metallic fragment.[28c] The nonplanar structure was explained in terms of the highly anionic character of the C_2H_2 fragment in the tungsten complex.[28c] This is not the case in the niobocene systems under consideration; therefore, we restricted our study to the in-plane migration of H.

Energies and geometries of the transition structures $TS1x^{CO}$ and $TS1n^{CO}$ are very similar. $TS1x^{CO}$ is reached from $4x^{CO}$ with an energy barrier of 30.0 kcal/mol, and $TS1n^{CO}$ lies 30.5 kcal/mol above $4n^{CO}$. These transition states have a product-like nature, with the migrating H almost transferred to $C_α$. The topological analysis of the electron density confirms this fact. A bond critical point was found between the α-carbon and the hydrogen atom, whereas such a bond critical point does not appear between the β-carbon and the hydrogen atom.

The next step in the 1,2-mechanism might be the slippage of the $η^2(C,H)$-alkyne-containing intermediate to form the more stable π-alkyne-containing product (B^{CO} → 5^{CO}). Indeed, we located a transition state for this process ($TS2^{CO}$; Figure 8). Because of the very small differences found between the *exo* and *endo* isomers in the niobocene carbonyl compounds, we only considered the alkyne reorganization for the slightly more stable *exo* isomer. The transition state $TS2x^{CO}$ is found only 0.7 kcal/mol above the intermediate. It is worth noting that in Figure 8 the geometry of $TS2x^{CO}$ shows a less distorted alkyne fragment than in Bx^{CO}. The Nb–$C_α$ and particularly the Nb–H distances are lengthened on going from **B** to **TS2**. A bond critical point between Nb and H was not found in $TS2x^{CO}$, but such a point was located for the Nb–$C_α$ bond. Thus, this transition state might be described as containing a σ $η^1$-alkyne struc-

(34) Olivan, M.; Clot, E.; Eisenstein, O.; Caulton, K. G. *Organometallics* **1998**, *17*, 3091.
(35) Bader, R. F. W. *Atoms in Molecules: A Quantum Theory*; Oxford University Press: New York, 1990.
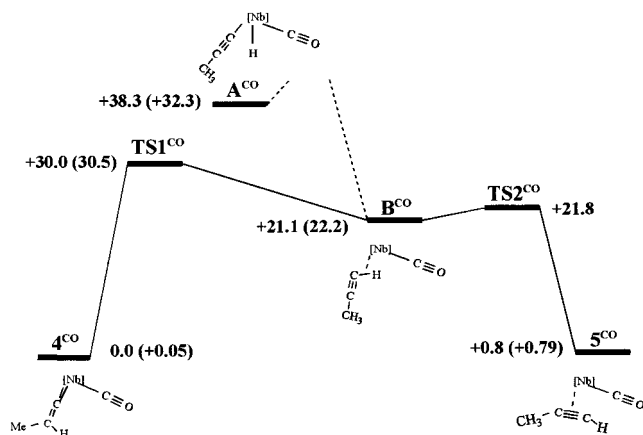
Figure 9. Potential energy profile (kcal mol^{-1}) for isomerization of *exo*-[NbCp$_2$(=C=CHCH$_3$)(CO)]$^+$ to *exo*-[NbCp$_2$-(HC≡CCH$_3$)(CO)]$^+$. Values in parentheses are calculated energies for *endo* isomers.
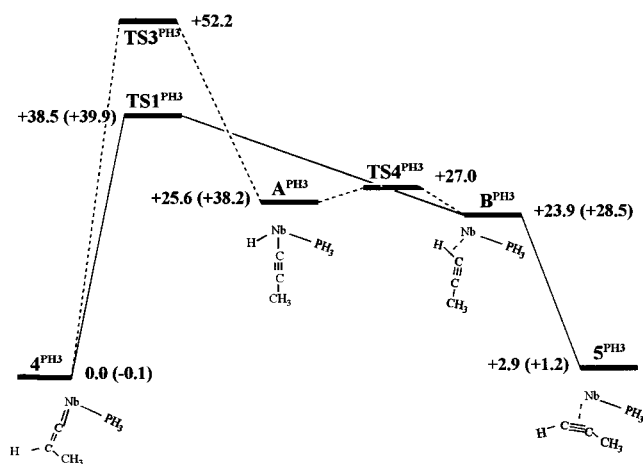
Figure 10. Potential energy profile (kcal mol^{-1}) for isomerization of *endo*-[NbCp$_2$(=C=CHCH$_3$)(PH$_3$)]$^+$ to *endo*-[NbCp$_2$(HC≡CCH$_3$)(PH$_3$)]$^+$. Values in parentheses are calculated energies for *exo* isomers.

ture. The very low energy barrier calculated for the process $\eta^2(C,H)$-alkyne → $\eta^2(C,C)$-alkyne shows that the **B** species are not very stable minima and suggests that the existence or nonexistence of the σ-coordinated η^2-(C,H)-alkyne as a reaction intermediate in the 1,2-mechanism will depend on the particular nature of the system. A slight destabilization of these intermediates causes the 1,2-mechanism to pass from a two-step process to a concerted reaction.

The calculated potential energy profile for the η^1-vinylidene → η^2-alkyne rearrangement in the niobocene carbonyl system is presented in Figure 9. The energies of the hydrido alkynyl intermediates are above those of the transition structures **TS1**^{CO}; thus, the 1,3-mechanism can be discarded for the **4**^{CO} → **5**^{CO} isomerization process. For this reason, we did not explore the reaction path for the 1,3-hydrogen migration.

The energetic profile obtained for the phosphine-containing niobocene system is depicted in Figure 10. With regard to the 1,2-mechanism, the two transition states (**TS1x**^{PH_3} and **TS1n**^{PH_3}; Figure 8) for the formation of $\eta^2(C,H)$-alkyne intermediates from the corresponding vinylidene complexes (**4**^{PH_3} → **B**^{PH_3}) were located. Although the geometries of both are very

similar to those found for the carbonyl system, there is a significant difference between the carbonyl- and phosphine-containing niobocenes: **TS1x**^{PH_3} and **TS1n**^{PH_3} lie 40.0 and 38.5 kcal/mol above the vinylidene structures, whereas **TS1**^{CO} species are reached with an energy barrier of 30 kcal/mol. The replacement of the carbonyl ligand by a less π-acid ligand appreciably increases the energy barrier of the 1,2-migration. We have already discussed the fact that when the CO ligand is replaced by PH$_3$, the electron density at the vinylidene C$_\alpha$ atom increases due to the enhancement of the metal back-donation. During the migration process this interaction must vanish to form the new C−H bond. Thus, the strongest interaction determines that the hydrogen migration would be more unfavorable. We did not determine the transition state for the next step of the 1,2-mechanism: the slippage process of the alkyne ligand (**B**^{PH_3} →**5**^{PH_3}). It is expected that this last step will take place with a low energy barrier, as found for the carbonyl system, and it should not be the rate-determining step in this mechanism.

In the potential energy surface of the phosphine-containing niobocene system the *endo* hydrido alkynyl intermediate **An**^{PH_3} was found to be energetically very close to the $\eta^2(C,H)$-alkyne-containing intermediate and more than 10 kcal/mol below the transition state **TS1**^{PH_3}. Thus, in this case the 1,3-mechanism could be operative. The search for a transition state that defines the 1,3-hydrogen migration led to the structure **TS3n**^{PH_3} (Figure 8), which is found 52.2 kcal/mol above the vinylidene species. This value clearly indicates that the **4**^{PH_3}→**A**^{PH_3} process is kinetically unfavorable with respect to the 1,2-migration. The **TS3n**^{PH_3} structure was unequivocally assigned as a transition state by a numerical calculation of its Hessian matrix.

The geometry of the transition state **TS3n**^{PH_3} is different from those of the previously reported transition states for the 1,3-hydrogen shift.[28b,c] The main difference is found in the metal−C$_\alpha$−C$_\beta$ angle (77.4° in **TS3n**^{PH_3}, 162.3° in RhCl(PH$_3$)$_2$(C=CH$_2$)[28b]). In the Rh(I) transition state the migrating H interacts simultaneously with Rh, C$_\alpha$, and C$_\beta$. A close look at the geometric parameters in Figure 8 and the topological analysis of the charge density shows that in **TS3n**^{PH_3} the hydrogen interacts only with the C$_\beta$ atom but the metal interacts simultaneously with both C$_\alpha$ and C$_\beta$ atoms. If we investigate the reverse process, i.e., from **A**^{PH_3} to **4**^{PH_3}, it could very well be considered as an insertion of the alkynyl ligand into the Nb−H bond rather than a 1,3-hydrogen shift. It is interesting to note that a C$_\alpha$−P interaction is developing in **TS3n**^{PH_3}, characterized by a bond critical point in the charge density. This interaction is probably involved in the stabilization of the transition state structure.

The very close energies of the hydrido alkynyl **An**^{PH_3} and $\eta^2(C,H)$-alkyne-containing **Bn**^{PH_3} intermediates prompted us to study their interconversion. A transition state for this process, **TS4n**^{PH_3} (Figure 8), was located only 1.4 kcal/mol above **An**^{PH_3}. The topological analysis of the electron density shows that in this transition state the hydrogen atom is interacting simultaneously with the metal atom and the α-carbon. The very low barrier found for the oxidative addition (and its reverse reductive elimination) of the C−H bond in this system
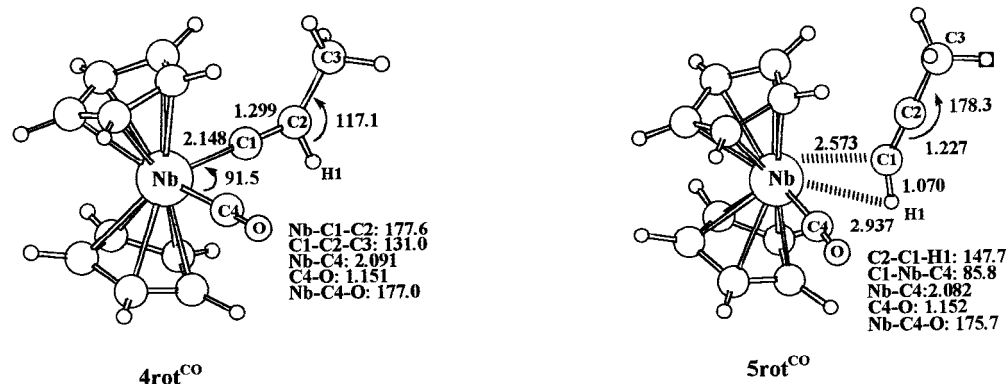
Figure 11. Partially optimized B3LYP structures (Å, deg) for rotation of vinylidene and alkyne ligands in [NbCp$_2$(=C=CHCH$_3$)(CO)]$^+$ and [NbCp$_2$(HC≡CCH$_3$)(CO)]$^+$, respectively.

suggests that hydrido alkynyl and $\eta^2(C,H)$-alkyne-containing species coexist and interconvert easily.

Our theoretical study has shown that in both the niobocene−carbonyl and the niobocene−phosphine systems the vinylidene → alkyne isomerization takes place by the 1,2-mechanism. The different experimental behaviors of **4a,c** and **4d** should be understood on the basis of kinetic effects rather than thermodynamics, as we suggested in the previous section. The difference of almost 10 kcal/mol found in the activation barrier of the vinylidene → $\eta^2(C,H)$-alkyne step justifies the experimental findings. Moreover, the calculated energy barrier of the rate-determining step (30 kcal/mol) is in accordance with the experimental conditions under which the **4a,c** → **5a,c** isomerization occurs (1−2 days, room temperature).

***exo → endo* Interconversion.** Up to now we have considered the isomerization reaction of the *exo* (*endo*) vinylidene to the *exo* (*endo*) alkyne species. It remains to be clarified as to how the *exo* and *endo* isomers are able to interconvert. With this aim in mind, we performed an estimation of the rotational barrier of the vinylidene and alkyne carbonyl species. The structures of the two complexes with the vinylidene and alkyne ligands rotated 90° from the orientation they adopt in the minima were partially optimized, with the ligands forced to remain in the rotated orientation (**4rot**^{CO} and **5rot**^{CO}, respectively; Figure 11).

The vinylidene-rotated structure is found 27.9 kcal/mol above the minimum **4x**^{CO}. This value gives an estimation of the rotational barrier. The high energetic cost of the rotation does not seem to be related to steric effects, since the methyl substituent is relatively far from the cyclopentadienyl rings. Thus, electronic factors should be responsible for this high rotation barrier. Vinylidene holds two nonequivalent π-acceptor orbitals: an empty π orbital in the CCH plane and a π^* orbital, which is higher in energy, in the perpendicular plane.[36] The only occupied d orbital of the d^2 [NbCp$_2$-(CO)]$^+$ metallic fragment lies in the plane that contains the vinylidene ligand and is perpendicular to the axis that joints the two Cp rings.[37] This orbital back-donates electron density to the π orbital in the minima **4**^{CO} and to π^* in the rotated structure **4rot**^{CO}. The π back-

donation diminishes with the rotation, as indicated by the evolution of the geometrical parameters (Figures 6 and 11). The same effect causes the high rotational barrier found for the dihydrogen ligand in dihydrogen niobocene complexes.[38]

To estimate the rotational barrier for the alkyne-containing complex, we started the optimization with an $\eta^2(C,C)$-alkyne structure rotated by 90°. However, the geometry optimization process ended in the **5rot**^{CO} structure. It is worth noting that the coordination of the alkyne ligand in **5rot**^{CO} (Figure 11) could be better described as an η^1-alkyne species. The instability of the $\eta^2(C,C)$-alkyne-rotated structure clearly has a steric origin and is caused by the repulsion between the methyl substituent of the alkyne and the Cp rings of the metallic fragment. The alkyne ligand is forced to change its coordination mode when it rotates in order to minimize the steric contacts. **5rot**^{CO} is found 20.9 kcal/mol above the alkyne minimum. The energy and the geometry of this structure suggests that it could be the transition state for the rotation of the $\eta^2(C,H)$-alkyne intermediates, **B**^{CO}. In fact, the optimization of **Bx**^{CO} rotated by 90° around the C−H bond leads to a structure that is almost identical with that of **5rot**^{CO}. A three-step mechanism for the rotation of the $\eta^2(C,C)$-alkyne complex can be envisaged. In the first step the π-alkyne complex rearranges to the σ $\eta^2(C,H)$-alkyne complex. Then the $\eta^2(C,H)$-alkyne complex rotates with a very low barrier, and finally, the slippage of the σ $\eta^2(C,H)$-alkyne complex gives the other isomer of the $\eta^2(C,C)$-alkyne species.

The study of the rotational processes has shown that the rotational barriers for the vinylidene and alkyne ligands in niobocene systems are high. For the vinylidene (27.9 kcal/mol), the value is in the range of the activation barrier for the vinylidene → alkyne rearrangement. For the alkyne, the reaction intermediates, i.e., $\eta^2(C,H)$-alkyne species, are involved in the rotation. The *exo* and *endo* isomers of reactants and products do not interconvert directly but can interconvert along the vinylidene → η^2-alkyne reaction path. The $\eta^2(C,H)$ → $\eta^2(C,C)$ slippage is the key step in the interconversion between the *exo* and *endo* isomers.

(36) Kostic, N. M.; Fenske, R. F. *Organometallics* **1982**, *1*, 974.
(37) Lauher, J. W.; Hoffmann, R. J. *J. Am. Chem. Soc.* **1976**, *98*, 1729.

(38) Antiñolo, A.; Carrillo-Hermosilla, F.; Fajardo, M.; Garcia-Yuste, S.; Otero, A.; Camanyes, S.; Maseras, F.; Moreno, M.; Lledòs, A.; Lluch, J. M. *J. Am. Chem. Soc.* **1997**, *119*, 6107.

Concluding Remarks

In conclusion, the first general procedure to prepare (σ-alkynyl)niobocene complexes has been described. These complexes were chemically and electrochemically oxidized, and we have observed that the nature of the resulting products, radical alkynyl, vinylidene, or divinylidene species, depends on the substituent R on the alkynyl ligand, the nature of the ancillary ligand L, and the experimental conditions (temperature and solvent). The noteworthy feature of this work is the observation of a new vinylidene to alkyne isomerization in the coordination sphere of an early transition metal. Theoretical calculations have shown that in both niobocene−carbonyl and niobocene−phosphine systems, vinylidene and alkyne complexes are isoenergetic, a situation that is in marked contrast with the systems previously considered in theoretical studies. Although in niobocene−phosphine systems the η^2-alkyne form is slightly more destabilized than in niobocene−carbonyl systems, this fact does not justify the different experimental behavior observed between **4a**, **4c**, and **4d**. An inspection of the factors governing the relative stability of vinylidene−alkyne complexes suggests that while the electrophilicity of the vinylidene α-carbon plays a key role in a given metal system, other factors may be responsible for the relative stability when different transition-metal systems are compared. A theoretical study of the possible intramolecular mechanisms for the isomerization has shown that it takes place by a two-step 1,2-hydrogen shift mechanism. In the first step a $\sigma \eta^2(C,H)$-alkyne is formed by means of a 1,2-hydrogen migration from the β- to the α-carbon. The next step is the slippage process of the alkyne ligand from a $\sigma \eta^2$-(C,H) coordination to an $\eta^2(C,C)$ coordination. The different experimental behaviors exhibited by **4a**, **4c**, and **4d** are explained in terms of kinetic effects. The difference of almost 10 kcal/mol found in the activation barrier of the η^1-vinylidene → $\eta^2(C,H)$-alkyne step found on going from the carbonyl−niobocene to the phosphine−niobocene system justifies the experimental findings. Moreover, the theoretical study indicates that $\eta^2(C,H)$-alkyne intermediates are involved in the *exo* → *endo* interconversion. The *exo* and *endo* isomers of reactants and products do not interconvert directly but can easily interconvert along the η^1-vinylidene → η^2-alkyne reaction path. This fact suggests a three-step mechanism for rotation of the terminal alkyne: (i) rearrangement of $\eta^2(C,C)$-alkyne toward an $\eta^2(C,H)$-alkyne species, (ii) *exo*−*endo* interconversion with a low rotational barrier of the $\eta^2(C,H)$-alkyne species, and (iii) a new slippage of the $\eta^2(C,H)$-alkyne complex to the other $\eta^2(C,C)$-alkyne isomer.

Experimental Section

General Considerations. Nb(η^5-C$_5$H$_4$SiMe$_3$)$_2$(Cl)(CO) and Nb(η^5-C$_5$H$_4$SiMe$_3$)$_2$Cl(PMe$_2$Ph) were prepared by published methods.[4a] The synthesis of the alkynylmagnesium compounds Mg(C≡CR)$_2$ was performed by following a previously reported method.[39] All reactions were carried out under an inert atmosphere (argon) using standard Schlenk techniques. Solvents were freshly distilled from appropriate drying agents and degassed before use. Elemental analyses were performed

(39) Eisch, J. J.; Sanchez, R. *J. Organomet. Chem.* **1985**, *296*, C-27.

with a Perkin-Elmer 240 B microanalyzer. NMR spectra were recorded on a Varian Unity FT-300 instrument (^{1}H at 300 MHz, ^{13}C at 75 MHz). IR spectra were recorded as Nujol mulls between CsI plates or as a KBr mull (in the region 4000−200 cm^{-1}) on a Perkin-Elmer PE 833 IR spectrophotometer. Mass spectroscopic analyses were performed on a VG Autospec instrument (FAB techniques using NBA as matrix) or a Hewlett-Packard 5988A (m/z 50−1000) (chemical ionization techniques). Cyclic voltammetry was carried out in a standard three-electrode Tacussel UAP$_4$ unit cell. The reference electrode was saturated calomel (SCE), separated from the solution by a sintered-glass disk. The auxiliary electrode was a platinum wire. For all voltammetric measurements the working electrode was either a vitreous carbon or platinum electrode. For controlled-potential electrolysis, a mercury pool was used as the anode and a platinum plate as the cathode, the latter being separated from the solution by a sintered-glass disk. In all cases the electrolyte was a 0.2 M solution of tetrabutylammonium hexafluorophosphate or perchlorate in tetrahydrofuran. The electrolyses were performed with an Amel 552 potentiostat coupled to an Amel 721 electronic integrator. Electron spin resonance spectra were taken at room temperature on a Bruker ESP300 spectrometer. Field calibrations were made with DPPH ($g = 2.0034$).

Synthesis of Nb(η^5-C$_5$H$_4$SiMe$_3$)$_2$(C≡CPh)(CO) (2a). Method 1. To a mixture of Nb(η^5-C$_5$H$_4$SiMe$_3$)$_2$(Cl)(CO) (180 mg, 0.41 mmol) and Mg(C≡CPh)$_2$ (140 mg, 0.62 mmol) was added toluene and the resulting suspension stirred at room temperature for 7 h. The solvent was subsequently removed in vacuo and the residue extracted with hexane. The resulting green solution was evaporated to dryness to give an oily product that was identified as the alkynyl complex **2a** (169 mg, 0.34 mmol, 83%).

Method 2. To a mixture of both *endo* and *exo* isomers of the vinylidene complex [Nb(η^5-C$_5$H$_4$SiMe$_3$)$_2$(=C=CHPh)(CO)]-[BPh$_4$] (**4a[BPh$_4$]**; 30 mg, 0.04 mmol) and KO^{t}Bu (4.12 mg, 0.04 mmol) was added THF at 0 °C. The color of the reaction mixture changed from yellow to green. After it was stirred for 30 min at this temperature, the reaction mixture was stirred for a further 30 min at room temperatue and evaporated to dryness and pentane added. The resulting solution was again evaporated to dryness to give the alkynyl complex Nb(η^5-C$_5$H$_4$-SiMe$_3$)$_2$(C≡CPh)(CO) (18 mg, 0.04 mmol, 99%). N.B.: deprotonation of [Nb(η^5-C$_5$H$_4$SiMe$_3$)$_2$(=C=CHPh)(CO)][BF$_1$] (**4a[BF$_4$]**) and [Nb(η^5-C$_5$H$_4$SiMe$_3$)$_2$($\eta^2(C,C)$-HC≡CPh)(CO))]$^+$ (**5a**) under the same conditions, also gave the alkynyl complexes in good yields. IR: ν_{CO} 1920, $\nu_{C≡C}$ 2076 cm^{-1}. ^{1}H NMR (C$_6$D$_6$): δ 0.19 (s, 18H, SiMe$_3$), 4.70−4.80 (2H), 4.80−4.86 (2H), 4.90−5.00 (2H), 5.20−5.30 (2H) (m, C$_5$H$_4$SiMe$_3$), 6.90−7.00 (m, 1H, *p*-C$_6$H$_5$ of PhC≡C), 7.04−7.12 (m, 2H, *m*-C$_6$H$_5$ of PhC≡C), 7.50−7.60 (m, 2H, *o*-C$_6$H$_5$ of PhC≡C). ^{13}C{^{1}H} NMR (C$_6$D$_6$): δ 0.18 (SiMe$_3$), 92.26, 94.13, 98.59, 99.34, 101.34 (C$_5$H$_4$SiMe$_3$), 113.21 (Ph*C*≡C−Nb), 122.07 (PhC≡*C*−Nb), 123.53 (C-4), 124.67 (C-3 and C-5), 129.63 (C-1), 130.84 (C-2 and C-6) (phenyl group of PhC≡C), 255.87 (*C*O). MS chemical ionization (m/e (relative intensity)): 496 (7) (M$^+$, [Nb(η^5-C$_5$H$_4$SiMe$_3$)$_2$(C≡CPh)(CO)]$^+$), 468 (100) (M$^+$ − CO), 395 (39) (M$^+$ − C≡CPh), 367 (67) (M$^+$ − CO − C≡CPh).

Synthesis of Nb(η^5-C$_5$H$_4$SiMe$_3$)$_2$(C≡CSiMe$_3$)(CO) (2b). To a mixture of Nb(η^5-C$_5$H$_4$SiMe$_3$)$_2$(Cl)(CO) (210 mg, 0.49 mmol) and Mg(C≡CSiMe$_3$)$_2$ (210 mg, 0.97 mmol) was added toluene at room temperature. The resulting solution was stirred at 80 °C for 7 h, with the color of the reaction mixture changing from purple to dark green. The solvent was then evaporated in vacuo and the residue extracted with pentane. The resulting solution was again evaporated to dryness to give an oily product, which was identified as complex **2b** (230 mg, 0.47 mmol, 96%). IR: ν_{CO} 1927, $\nu_{C≡C}$ 2015 cm^{-1}. ^{1}H NMR (C$_6$D$_6$): δ 0.17 (s, 18H, C$_5$H$_4$Si*Me*$_3$), 0.32 (s, 9H, C≡CSi*Me*$_3$), 4.68−4.78 (4H), 4.86−4.94 (2H), 5.16−5.22 (2H) (m, C$_5$H$_4$-SiMe$_3$). ^{13}C{^{1}H} NMR (C$_6$D$_6$): δ 0.15 (C$_5$H$_4$Si*Me*$_3$), 1.80 (C≡

CSiMe_3), 92.30, 93.87, 98.76, 99.11, 101.32 (C_5H_4SiMe$_3$), 102.80 (Me$_3$SiC≡C−Nb), 129.28 (Me$_3$SiC≡C−Nb), 255.64 (CO). MS chemical ionization (m/e (relative intensity)): 493 (27) (M$^+$ + 1), 492 (18) (M$^+$, [Nb(η^5-C$_5$H$_4$SiMe$_3$)$_2$(C≡CSiMe$_3$)(CO)]$^+$), 477 (33) (M$^+$ − Me), 464 (18) (M$^+$ − CO), 395 (100) (M$^+$ − C≡CSiMe$_3$), 367 (21) (M$^+$ − CO − C≡CSiMe$_3$).

Synthesis of Nb(η^5-C$_5$H$_4$SiMe$_3$)$_2$(C≡C^{t}Bu)(CO) (2c). Method 1. The synthesis of the alkynyl complex **2c** was carried out by following the same method as described for **2a** and **2b** above. Thus, 320 mg (0.73 mmol) of Nb(η^5-C$_5$H$_4$SiMe$_3$)$_2$-(Cl)(CO) was treated with 260 mg (1.39 mmol) of Mg(C≡C^{t}Bu)$_2$ in toluene and the reaction mixture stirred at 80 °C for 7 h. The solvent was then removed in vacuo and the resulting solid washed twice with pentane at 0 °C. The combined washings were then evaporated to dryness to give the alkynyl complex **2c** as a green oil (330 mg, 0.69 mmol, 94%).

Method 2. To an equimolar mixture of [Nb(η^5-C$_5$H$_4$SiMe$_3$)$_2$-(=C=CH^{t}Bu)(CO)][BF$_4$] (**4c**[BF$_4$]; 100 mg, 0.18 mmol) and KO^{t}Bu (20 mg, 0.18 mmol) was added 10 mL of THF at 0 °C. A rapid color change from yellow to green was observed. The reaction mixture was stirred for 30 min at 0 °C and then for a further 30 min at room temperature. The solvent was then removed in vacuo and the residue extracted with pentane. The resulting solution was then evaporated to dryness to give the alkynyl complex **2c** (81 mg, 0.17 mmol, 95%). N.B.: when the same reaction was carried out using a mixture of both *endo* and *exo* isomers of [Nb(η^5-C$_5$H$_4$SiMe$_3$)$_2$(η^2(C,C)-HC≡C^{t}Bu)-(CO)]$^+$ (**5c**), the same result was obtained and **2c** was isolated in good yield. IR: ν_{CO} 1910, $\nu_{C≡C}$ 2093 cm^{-1}. ^{1}H NMR (C$_6$D$_6$): δ 0.20 (s, 18H, SiMe$_3$), 1.35 (s, 9H, C≡CCMe$_3$), 4.70−4.77 (2H), 4.77−4.82 (2H), 4.92−5.00 (2H), 5.22−5.28 (2H), (m, C$_5$H$_4$-SiMe$_3$). ^{13}C{^{1}H} NMR (C$_6$D$_6$): δ 0.19 (SiMe$_3$), 29.67 [C≡CC(CH$_3$)$_3$], 32.94 [C≡CC(CH$_3$)$_3$], 91.88, 93.60, 98.81, 98.81, 101.98 (C$_5$H$_4$SiMe$_3$), 112.50 (^{t}BuC≡C−Nb), 129.75 (^{t}BuC≡C−Nb), 257.85 (CO). MS chemical ionization (m/e (relative intensity)): 477 (44) (M$^+$ + 1), 476 (29) (M$^+$, [Nb(η^5-C$_5$H$_4$-SiMe$_3$)$_2$(C≡C^{t}Bu)(CO)]$^+$), 461 (42) (M$^+$ − Me), 448 (63) (M$^+$ − CO), 395 (100) (M$^+$ − C≡C^{t}Bu), 367 (17) (M$^+$ − CO − C≡C^{t}Bu).

Synthesis of Nb(η^5-C$_5$H$_4$SiMe$_3$)$_2$(C≡CPh)(PMe$_2$Ph) (2d). Method 1. To a mixture of Nb(η^5-C$_5$H$_4$SiMe$_3$)$_2$(Cl)(PMe$_2$Ph) (130 mg, 0.24 mmol) and Mg(C≡CPh)$_2$ (110 mg, 0.49 mmol) was added toluene and the resulting suspension stirred at room temperature for 4 h. The solvent was removed in vacuo and the residue extracted with pentane. The resulting red solution was evaporated to dryness to give an oily red solid that was subsequently washed with pentane at −80 °C. The red precipitate that was formed was identified as **2d** (100 mg, 0.16 mmol, 71%).

Method 2. To a mixture of both *endo* and *exo* isomers of the vinylidene complex [Nb(η^5-C$_5$H$_4$SiMe$_3$)$_2$(=C=CHPh)(PMe$_2$-Ph)][BF$_4$] (**4d**; 30 mg, 0.04 mmol) and KO^{t}Bu (4.12 mg, 0.04 mmol) was added THF at 0 °C, with the color changing from yellow to dark red. The reaction mixture was stirred for 30 min at 0 °C and then for a further 30 min at room temperature. The mixture was evaporated to dryness and the residue extracted several times with pentane. The resulting solution was again evaporated to dryness to give the alkynyl complex Nb(η^5-C$_5$H$_4$SiMe$_3$)$_2$(C≡CPh)(PMe$_2$Ph) (**2d**; 21.22 mg, 0.035 mmol, 88%). IR (KBr): $\nu_{C≡C}$ 2035 cm^{-1}. ^{1}H NMR (C$_6$D$_6$): δ 0.20 (s, 18H, SiMe$_3$), 1.36 [d, $^2J_{P-H}$ = 7.69 Hz, 6H, P(CH$_3$)$_2$Ph], 4.40−4.50 (2H), 4.55−4.70 (4H), 5.30−5.40 (2H) (m, C$_5$H$_4$-SiMe$_3$), 6.90−7.30 (m, 6H), 7.43−7.55 (m, 4H) (C$_6$H$_5$ groups of PhC≡C and PMe$_2$Ph). ^{13}C{^{1}H} NMR (C$_6$D$_6$): δ 0.52 (SiMe$_3$), 18.28 [d, $^1J_{P-C}$ = 23.8 Hz, P(CH$_3$)$_2$Ph], 90.34, 91.79, 95.27, 97.19, 101.96 (C$_5$H$_4$SiMe$_3$), 100.82 (PhC≡C), 104.58 (broad, PhC≡C−Nb), 123.18 (C-4), 128.96 (C-3 and -5), 129.47 (C-2 and -6), 129.70 (C-1) (phenyl group of PhC≡C), 128.88 (d, $^3J_{P-C}$ = 11.90 Hz, C-3 and -5), 129.47 (s, C-4), 130.32 (d, ^2J = 8.24 Hz, C-2 and -6), 142.38 (d, $^1J_{P-C}$ = 29.30 Hz, C-1) (phenyl group of PMe$_2$Ph). FAB MS (m/e (relative intensity)): 607 (77) (M$^+$ + 1), 606(22) (M$^+$, [Nb(η^5-C$_5$H$_4$SiMe$_3$)$_2$)(C≡CPh)(PMe$_2$Ph)]$^+$),

468 (18) (M$^+$ − PMe$_2$Ph), 367 (50) (M$^+$ − PMe$_2$Ph − C≡CPh). Anal. Calcd for C$_{32}$H$_{42}$Si$_2$NbP: C, 63.35; H, 6.98. Found: C, 63.20; H, 6.90.

Synthesis of Nb(η^5-C$_5$H$_4$SiMe$_3$)$_2$(C≡CPh)(P(OEt$_3$)) (2e). To a mixture of Nb(η^5-C$_5$H$_4$SiMe$_3$)$_2$(Cl)(P(OEt)$_3$)(Cl) (560 mg, 0.98 mmol) and Mg(C≡CPh)$_2$ (660 mg, 2.90 mmol) was added toluene and the resulting suspension stirred at room temperature for 3 h. The solvent was removed in vacuo and the residue extracted with pentane. The resulting red solution was evaporated to dryness to give an oily red solid. The solid was washed with pentane at −80 °C to give a red oily product, which was identified as **2d** (600 mg, 0.94 mmol, 96.5%). IR (KBr): $\nu_{C≡C}$ 2049 cm^{-1}. ^{1}H NMR (C$_6$D$_6$): δ 0.29 (s, 18H, SiMe$_3$), 1.06 [t, $^2J_{H-H}$ = 6.96 Hz, 9H, P(OCH$_2$CH$_3$)$_3$], 4.04 [dq, $^3J_{P-H}$ = 6.96 Hz, $^2J_{H-H}$ = 6.96 Hz, 6H, P(OCH$_2$CH$_3$)$_3$], 4.85−4.90 (2H), 4.90−5.00 (2H), 5.05−5.15 (2H), 5.50−5.60 (2H) (m, C$_5$H$_4$-SiMe$_3$), 6.85−6.95 (m, 3H), 7.30−7.40 (m, 2H) (C$_6$H$_5$ group of PhC≡C). ^{13}C{^{1}H} NMR (C$_6$D$_6$): δ 0.46 (SiMe$_3$), 16.42 [d, $^3J_{P-C}$ = 5.49 Hz, P(OCH$_2$CH$_3$)$_3$], 61.26 [d, $^2J_{P-C}$ = 5.49 Hz, P(OCH$_2$-CH$_3$)$_3$], 91.19, 92.33, 94.01, 97.46, 103.36 (C$_5$H$_4$SiMe$_3$), 100.78 (PhC≡C), 104.40 (broad, PhC≡C−Nb), 123.09 (C-4), 127.05 (C-3 and -5), 129.33 (C-2 and -6), 133.90 (C-1) (phenyl group of PhC≡C). FAB MS (m/e (relative intensity)): 635 (33) (M$^+$ + 1), 634 (11) (M$^+$, [Nb(η^5-C$_5$H$_4$SiMe$_3$)$_2$(C≡CPh)(P(OEt)$_3$)]$^+$), 468 (19) [M$^+$ − P(OEt)$_3$]; 367 (68) [M$^+$ − P(OEt)$_3$ − C≡CPh].

Synthesis of Nb(η^5-C$_5$H$_5$)$_2$(C≡CSiMe$_3$)(CO) (2f). To a solution of the alkynyl complex Nb(η^5-C$_5$H$_4$SiMe$_3$)$_2$(C≡CSiMe$_3$)-(CO) (**2b**; 120 mg, 0.24 mmol) in THF at 0 °C was added 19.7 μL (15.6 mg, 0.48 mmol) of dry, freshly distilled MeOH and 121.80 μL (0.12 mmol) of a 1 M solution of the desilylating agent NBu$_4$F in THF. The mixture was stirred at 0 °C for 1 h and then for a further 1 h 45 min at room temperature. The solvent was then removed in vacuo and the red residue extracted with a mixture of toluene and diethyl ether (80/20). The resulting solution was left to stand overnight at −35 °C to precipitate various impurities. Subsequent filtration at this temperature gave a green solution, which was evaporated to dryness to give a green solid identified as Nb(η^5-C$_5$H$_5$)$_2$(C≡CSiMe$_3$)(CO) (70 mg, 0.20 mmol, 80%). IR (KBr): ν_{CO} 1897, $\nu_{C≡C}$ 2004 cm^{-1}. ^{1}H NMR (C$_6$D$_6$): δ 0.34 (s, 9H, C≡CSiMe$_3$), 4.65 (s, 10H, C$_5$H$_5$). ^{13}C{^{1}H} NMR (C$_6$D$_6$): δ 1.96 [C≡CSi-(CH$_3$)$_3$], 92.28 (C$_5$H$_5$), 92.16 (Me$_3$SiC≡C−Nb), 129.02 (Me$_3$SiC≡C−Nb). The CO carbon is not observed. MS chemical ionization (m/e (relative intensity)): 348 (83) (M$^+$, [Nb(η^5-C$_5$H$_5$)$_2$(C≡CSiMe$_3$)(CO)]$^+$), 333 (100) (M$^+$ − Me), 320 (70) (M$^+$ − CO), 251 (38) (M$^+$ − C≡CSiMe$_3$), 223 (40) (M$^+$ − CO − C≡CSiMe$_3$). Anal. Calcd for C$_{16}$H$_{19}$NbOSi: C, 55.18; H, 5.50. Found: C, 54.91; H, 5.54.

Synthesis of Nb(η^5-C$_5$H$_5$)$_2$(C≡CH)(CO) (2g). To a mixture of the alkynyl complex Nb(η^5-C$_5$H$_5$)$_2$(C≡CSiMe$_3$)(CO) (**2f**; 210 mg, 0.60 mmol) and K$_2$CO$_3$ (50 mg, 0.36 mmol) was added 3 mL of dry, freshly distilled methanol at 0 °C. The mixture was stirred at this temperature for 30 min and then for a further 1 h at room temperature. The mixture was then left to stand for 30 min and filtered to separate the remaining K$_2$CO$_3$. The solvent was evaporated in vacuo and the resulting green solid washed with cold diethyl ether (−30 to −40 °C). N.B.: the green product often appears contaminated with an orange solid that is insoluble in toluene at −40 °C and which has yet to be identified. Thus, when the impure compound **2g** is dissolved in the minimum amount of toluene and left to stand at −40 °C for 12 h, a red precipitate and a green solution are obtained. After filtration and evaporation of the filtrate to dryness, the terminal alkynyl complex **2g** is obtained as a green micro-crystalline solid (64 mg, 0.23 mmol, 40%). IR (KBr): ν_{CO} 1892, $\nu_{C≡C}$ 2044, $\nu_{≡C-H}$ 3264 cm^{-1}. ^{1}H NMR (C$_6$D$_6$): δ 2.53 (s, 1H, C≡CH), 4.72 (s, 10H, C$_5$H$_5$). ^{13}C{^{1}H} NMR (C$_6$D$_6$): δ 92.16 (C$_5$H$_5$), 92.31 (HC≡C−Nb), 107.85 (HC≡C−Nb). The CO carbon is not observed. FAB MS (m/e (relative intensity)): 277 (81) (M$^+$ + 1), 276 (13) (M$^+$, [Nb(η^5-C$_5$H$_5$)$_2$(C≡CH)(CO)]$^+$), 248 (50) (M$^+$ − CO), 251 (13) (M$^+$ − C≡CH), 223 (100) (M$^+$ − CO

– C≡CH). Anal. Calcd for $C_{13}H_{11}NbO$: C, 56.54; H, 3.98. Found: C, 56.49; H, 4.05.

Synthesis of [Nb(η^5-C$_5$H$_4$SiMe$_3$)$_2$(C≡CPh)(PMe$_2$Ph)]-[BPh$_4$] (3d). To a solution of Nb(η^5-C$_5$H$_4$SiMe$_3$)$_2$(C≡CPh)-(PMe$_2$Ph) (**2d**; 80 mg, 0.13 mmol) in dichloromethane at −30 °C was added [Fe(η^5-C$_5$H$_5$)$_2$][BPh$_4$] (66 mg, 0.13 mmol), with the color of the solution quickly changing from dark to bright light red. After the mixture was stirred for 45 min, pentane was slowly added at −30 °C and a red crystalline solid precipitated. The solid was filtered off and washed several times with pentane at the same temperature and dried in vacuo. The resulting red crystals were identified as the paramagnetic complex **3d** (60 mg, 0.065 mmol, 50%). IR (KBr): $\nu_{C≡C}$ 2034 cm^{-1}. FAB MS (*m/e* (relative intensity)): 607 (57) (M$^{•+}$ + 1), 606 (100) (M$^{•+}$, [Nb(η^5-C$_5$H$_4$SiMe$_3$)$_2$ (C≡CPh)-(PMe$_2$Ph)]$^{•+}$), 468 (41) (M$^{•+}$ − PMe$_2$Ph), 367 (31) (M$^{•+}$ − PMe$_2$-Ph − C≡CPh). Anal. Calcd for $C_{56}H_{62}BNbPSi_2$: C, 72.64; H, 6.75. Found: C, 72.60; H, 6.85.

Synthesis of [Nb(η^5-C$_5$H$_4$SiMe$_3$)$_2$(=C=CHPh)(CO)]$^+$ (4a). Method 1. To an equimolar mixture of Nb(η^5-C$_5$H$_4$SiMe$_3$)$_2$-(C≡CPh)(CO) (**2a**; 170 mg, 0.34 mmol) and [FeCp$_2$][BPh$_4$] (173 mg, 0.34 mmol) was added 30 mL of CH$_2$Cl$_2$ at −30 °C. The solution was stirred for 2 h 30 min while the temperature was slowly increased to −10 °C. The mixture was then stirred for a further 1 h between −10 and 10 °C. After this time the solvent was evaporated to dryness to give an orange oily residue that, after washing several times with diethyl ether, gave a yellow solid, which was subsequently identified as a 1:1 mixture of both *exo* and *endo* isomers of [Nb(η^5-C$_5$H$_4$-SiMe$_3$)$_2$(=C=CHPh)(CO)][BPh$_4$] (190 mg, 0.23 mmol, 68%). Spectroscopic data for **3a**[BPh$_4$] are as follows. IR (Nujol): $\nu_{C=C}$ vinylidene 1620, ν_{CO} 2054 cm^{-1}. ^{1}H NMR (CD$_3$CN): δ 0.20, 0.23 (s, 18H, SiMe$_3$, both isomers), 5.92–5.98 (2H), 6.00–6.04 (2H), 6.04–6.08 (2H), 6.10–6.14 (2H), 6.14–6.18 (2H), 6.18–6.26 (6H) (m, C$_5$H$_4$SiMe$_3$, both isomers), 6.78–6.88 (m, 8H, *p*-C$_6$H$_5$), 6.92–7.04 (m, 16H, *m*-C$_6$H$_5$), 7.20–7.32 (m, 16H, *o*-C$_6$H$_5$) (phenyl group of BPh$_4$$^-$), 7.10–7.20 (m, 4H, *m*-C$_6$H$_5$−C=C=Nb), 7.32–7.42 (s, 1H, =C*H*Ph, and m, 6H, *p*- and *o*-C$_6$H$_5$−C=C=Nb), 7.63 (s, 1H, =C=C*H*Ph). Anal. Calcd for $C_{49}H_{52}BNbOSi_2$: C, 72.05; H, 6.42. Found: C, 71.90; H, 6.40.

Method 2. To a solution of Nb(η^5-C$_5$H$_4$SiMe$_3$)$_2$(C≡CPh)(CO) (**2a**; 120 mg, 0.24 mmol) in diethyl ether was added 35.6 μL (39 mg, 0.24 mmol) of HBF$_4$·2Et$_2$O (solution in Et$_2$O) at −30 °C. The reaction mixture was stirred while the temperature of the solution was slowly increased to 25 °C. The product precipitated as a yellow solid, which was isolated by filtration and washed twice with the same solvent. This solid was subsequently identified as a 1:1 mixture of both *exo* and *endo* isomers of the complex [Nb(η^5-C$_5$H$_4$SiMe$_3$)$_2$(=C=CHPh)(CO)]-[BF$_4$] (**4a**[BF$_4$]; 120 mg, 0.20 mmol, 86%). Spectroscopic data for **4a**[BF$_4$] are as follows. IR (Nujol): $\nu_{C=C}$ vinylidene 1641, ν_{CO} 2073 cm^{-1}. ^{1}H NMR (CD$_3$CN): δ 0.20, 0.23 (s, 18H, SiMe$_3$, both isomers), 5.96–6.02 (2H), 6.02–6.10 (4H), 6.10–6.16 (2H), 6.16–6.20 (2H), 6.20–6.30 (6H) (m, C$_5$H$_4$SiMe$_3$, both isomers), 7.10–7.22 (m, 4H, *m*-C$_6$H$_5$C=C=Nb), 7.24–7.42 (m, 6H, *p*- and *o*-C$_6$H$_5$C=C=Nb), 7.38, 7.63 (s, 1H, =C=C*H*Ph, both isomers). The proportion of isomers initially observed when the ^{1}H NMR spectrum was acquired in CD$_3$COCD$_3$ at −70 °C was 2:5. All the NMR data in this case are as follows. ^{1}H NMR (CD$_3$COCD$_3$, −70 °C, *major isomer*): δ 0.22 (s, 18H, SiMe$_3$), 6.30–6.50 (4H), 6.50–6.70 (4H), (m, C$_5$H$_4$SiMe$_3$), 7.20–7.44 (m, 5H, phenyl group of C$_6$H$_5$−C=C=Nb), 7.86 (s, 1H, =C=C*H*Ph). ^{1}H NMR (CD$_3$COCD$_3$, −70 °C, *minor isomer*): δ 0.26 (s, 18H, SiMe$_3$), 6.20–6.30 (2H), 6.30–6.50 (2H), 6.50–6.70 (2H), 6.70–6.90 (2H), (m, C$_5$H$_4$SiMe$_3$), 7.20–7.44 [m, 5H, phenyl group of (C$_6$H$_5$)HC=C=Nb], 7.74 (s, 1H, =C=C*H*Ph). ^{13}C{^{1}H} NMR (CD$_3$COCD$_3$, −70 °C, mixture of both *endo* and *exo* isomers): δ −1.32, −1.03 (SiMe$_3$), 103.96, 104.32, 105.20, 105.53, 105.66, 106.90, 107.03, 107.64 (C$_5$H$_4$SiMe$_3$), 126.58, 127.03 (*p*-C$_6$H$_5$), 127.99, 128.09 (*m*-C$_6$H$_5$), 128.98, 129.16 (*o*-C$_6$H$_5$), 133.98, 135.44 (C$_{ipso}$) (phenyl groups of C$_6$H$_5$HC=C=Nb), 132.35,

132.85 (Nb=C=*C*), 213.74, 214.44 (CO), 377.97, 378.39 (Nb=*C*=C). FAB MS (*m/e* (relative intensity)): 497 (100) (M$^+$, [Nb-(η^5-C$_5$H$_4$SiMe$_3$)$_2$(CCHPh)(CO)]$^+$), 469 (27) (M$^+$ − CO), 395 (62) (M$^+$ - CCHPh), 367 (69) (M$^+$ - CO − CCHPh). Anal. Calcd for $C_{25}H_{32}BF_4NbOSi_2$: C, 51.40; H, 5.48. Found: C, 51.38; H, 5.50.

Synthesis of [Nb(η^5-C$_5$H$_4$SiMe$_3$)$_2$(=C=CH$_2$)(CO)][BPh$_4$] (4h). The oxidation of the Nb(III) complex **2b**, described above, always yielded an unexpected product that was difficult to isolate. The best results were obtained when 180 mg (0.36 mmol) of **2b**, Nb(η^5-C$_5$H$_4$SiMe$_3$)$_2$(C≡CSiMe$_3$)(CO), was treated with 182 mg (0.36 mmol) of [FeCp$_2$][BPh$_4$] in THF at −20 °C. The reaction mixture was stirred for 10 min between −20 and 0 °C and for a further 15 min at this temperature. The resulting red-brown solution was evaporated to dryness to give an oily green residue, which was then washed several times with diethyl ether at 0 °C. A gray solid was finally isolated and identified as the terminal monovinylidene compound [Nb-(η^5-C$_5$H$_4$SiMe$_3$)$_2$(=C=CH$_2$)(CO)][BPh$_4$] (**4e**; 80 mg, 0.10 mmol, 30%). All attempts at recrystallization of this complex resulted in decomposition. IR (Nujol): $\nu_{C=C}$ vinylidene 1620, ν_{CO} 2042 cm^{-1}. ^{1}H NMR (CD$_3$CN): δ 0.25 (s, 18H, SiMe$_3$), 5.94–6.01 (4H), 6.01–6.05 (2H), 6.08–6.12 (2H) (m, C$_5$H$_4$SiMe$_3$), 6.14, 6.15 (s, 1H, H$_2$C=C=Nb), 6.79–6.88 (4H, *p*-C$_6$H$_5$), 6.94–7.04 (8H, *m*-C$_6$H$_5$), 7.21–7.32 (8H, *o*-C$_6$H$_5$) (phenyl groups of BPh$_4$$^-$). ^{13}C{^{1}H} NMR (CD$_3$CN): δ −0.10 (SiMe$_3$), 104.39, 104.91, 106.08, 107.66, 109.79 (C$_{ipso}$) (C$_5$H$_4$SiMe$_3$), 118.64 (Nb=C=*C*H$_2$), 122.73, 126.56, 136.73 (phenyl groups of BPh$_4$$^-$), 164.78 (C$_{ipso}$ of phenyl groups of BPh$_4$$^-$, q, $J_{^{13}C−^{11}B}$ = 49 Hz). Signals corresponding to carbons of CO and Nb=*C*=CH$_2$ are not observed. FAB MS (*m/e* (relative intensity)): 421 (100) (M$^+$, [Nb(η^5-C$_5$H$_4$SiMe$_3$)$_2$(CCH$_2$)(CO)]$^+$), 395 (41) (M$^+$ - CCH$_2$), 393 (35) (M$^+$ − CO), 367 (72) (M$^+$ − CCH$_2$ − CO). Simulation of the isotopic composition of M$^+$ was identical with the experimental result. Anal. Calcd for $C_{43}H_{48}BNbOSi_2$: C, 69.72; H, 6.53. Found: C, 69.77; H, 6.55.

Synthesis of [Nb(η^5-C$_5$H$_4$SiMe$_3$)$_2$(=C=CH^{t}Bu)(CO)]$^+$ (4c). Method 1. To an equimolar mixture of Nb(η^5-C$_5$H$_4$SiMe$_3$)$_2$-(C≡C^{t}Bu)(CO) (**2c**; 70 mg, 0.15 mmol) and [FeCp$_2$][BPh$_4$] (74 mg, 0.15 mmol) was added 20 mL of CH$_2$Cl$_2$ at −30 °C. The solution was then slowly warmed to −10 °C over 2 h 30 min and then to 10 °C over a further 1 h. After this time the solvent was removed in vacuo and the resulting oily brown mixture washed twice with diethyl ether at 0 °C to give a pale brown precipitate, which was subsequently identified as a single isomer of the compound [Nb(η^5-C$_5$H$_4$SiMe$_3$)$_2$(=C=CH^{t}Bu)(CO)]-[BPh$_4$] (**4c**[BPh$_4$]; 56 mg, 0.07 mmol, 48%). Dimerization to the divinylidene complex *was not observed in any case*, even when the reaction was performed under different reaction conditions (solvents, temperature, and concentration). Spectroscopic data for **4c**[BPh$_4$] are as follows. ^{1}H NMR (CD$_3$CN): δ 0.24 (s, 18H, SiMe$_3$), 1.08 (s, 9H, ^{t}Bu), 5.80–5.86 (2H), 5.88–5.94 (2H), 5.94–6.00 (2H), 6.20–6.26 (2H) (m, C$_5$H$_4$SiMe$_3$), 6.53 (s, 1H, =C=C*H*^{t}Bu), 6.78–6.88 (m, 4H, *p*-C$_6$H$_5$), 6.92–7.04 (m, 8H, *m*-C$_6$H$_5$), 7.20–7.30 (m, 8H, *o*-C$_6$H$_5$) (phenyl group of BPh$_4$$^-$). Anal. Calcd for $C_{47}H_{56}BNbOSi_2$: C, 70.84; H, 7.08. Found: C, 70.89; H, 7.05.

Method 2. To a solution of Nb(η^5-C$_5$H$_4$SiMe$_3$)$_2$(C≡C^{t}Bu)-(CO) (**2c**; 200 mg, 0.42 mmol) in 20 mL of diethyl ether at −40 °C was added 62 μL (0.42 mmol) of HBF$_4$·2Et$_2$O (solution in Et$_2$O). This solution was stirred for 2 h, with the color changing from green to orange, until the temperature had reached −5 °C. The product precipitated as a yellow solid, which was isolated by filtration and washed three times with the same solvent. The resulting solid was identified as [Nb(η^5-C$_5$H$_4$-SiMe$_3$)$_2$(=C=CH^{t}Bu)(CO)][BF$_4$] (**4c**[BF$_4$]; 100 mg, 0.18 mmol, 42%). Spectroscopic data for **4c**[BF$_4$] are as follows. IR (KBr): $\nu_{C=C}$ vinylidene 1626, ν_{CO} 2074 cm^{-1}. ^{1}H NMR (CD$_3$CN), δ 0.24 (s, 18H, SiMe$_3$), 1.08 (s, 9H, ^{t}Bu), 5.82–5.88 (2H), 5.90–5.96 (2H), 5.94–6.02 (2H), 6.22–6.28 (2H) (m, C$_5$H$_4$SiMe$_3$), 6.53 (s, 1H, =C=C*H*^{t}Bu'). ^{1}H NMR (CD$_3$COCD$_3$, −70 °C): δ 0.31 (s, 18H, SiMe$_3$), 1.13 (s, 9H, ^{t}Bu), 6.14 (2H), 6.22 (2H), 6.32 (2H),

6.58 (2H), (m, $C_5H_4SiMe_3$), 6.68 (s, 1H, =C=CH^tBu). ^{13}C{^{1}H} NMR (CD$_3$COCD$_3$, −70 °C): δ −0.13 (SiMe$_3$), 30.48 [C(CH_3)$_3$], 37.80 [C(CH$_3$)$_3$], 104.85, 105.09, 105.96, 107.96, 112.50 (C_5H_4-SiMe$_3$), 144.09 (Nb=C=C), 218.39 (CO). The signal corresponding to (Nb=C=C) is not observed. Anal. Calcd for C$_{23}$H$_{36}$BF$_4$NbOSi$_2$: C, 48.94; H, 6.43. Found: C, 48.90; H, 6.45.

Synthesis of [Nb($η^5$-C$_5$H$_4$SiMe$_3$)$_2$(=C=CHPh)(PMe$_2$Ph)]-[BF$_4$] (4d). To a solution of Nb($η^5$-C$_5$H$_4$SiMe$_3$)$_2$(C≡CPh)(PMe$_2$-Ph) (**2d**; 100 mg, 0.165 mmol) in diethyl ether at −30 °C was added 24.2 μL (27 mg, 0.165 mmol) of HBF$_4$·2Et$_2$O (solution in diethyl ether). The rapid formation of a yellow precipitate was observed. The solution was stirred for 30 min at this temperature and then left to stand. The yellow precipitate was filtered off, washed twice with diethyl ether, and dried in vacuo. The solid was identified as a 1:1 mixture of the *endo* and *exo* isomers of the cationic monovinylidene complex [Nb-($η^5$-C$_5$H$_4$SiMe$_3$)$_2$(=C=CHPh)(PMe$_2$Ph)][BF$_4$] (**4d**; 70 mg, 0.10 mmol, 61%). IR (KBr): $ν_{C=C}$ vinylidene 1622 cm^{-1}. ^{1}H NMR (CD$_3$CN): δ 0.15, 0.21 (s, 18H, SiMe$_3$), 1.79, 1.88 [d, $^2J_{P-H}$ = 9.15 Hz, 6H, PPh(CH_3)$_2$], 5.26−5.34 (2H), 5.48−5.56 (2H), 5.70−5.78 (6H), 5.78−5.86 (2H), 5.98−6.06 (2H), 6.12−6.22 (2H) (m, C$_5H_4$SiMe$_3$), 7.20−7.34 (m, 10H), 7.34−7.44 (m, 5H), 7.52−7.60 (m, 3H), 7.60−7.70 (m, 2H) [phenyl groups of (C$_6H_5$)HC=C=Nb and PMe$_2$Ph], 7.45, 7.69 (s, 1H, =C=CHPh). ^{13}C{^{1}H} NMR (CD$_3$CN, mixture of both *endo* and *exo* isomers): δ 0.00 (SiMe$_3$), 19.33 [d, $^1J_{P-C}$ = 32.04 Hz, P(CH_3)$_2$-Ph], 20.11 [d, $^1J_{P-C}$ = 30.52 Hz, P(CH_3)$_2$Ph], 101.18, 103.35, 103.87, 105.63, 106.99, 107.23, 108.12, 108.89, 111.34, 112.63 (C_5H_4SiMe$_3$), 128.01, 128.41 (C-4), 129.79, 129.95 (C-3 and -5), 131.49, 131.63 (C-2 and -6), 134.14, 136.36 (C-1) [phenyl groups of (C_6H_5)HC=C=Nb], 128.48 (d, $^3J_{P-C}$ = 10.68 Hz, C-3 and -5), 129.87 (d, $^3J_{P-C}$ = 12.20 Hz, C-3 and -5), 130.19, 131.04 (d, $^2J_{P-C}$ = 9.16 Hz, C-2 and -6), 131.49, 131.63 (s, C-4), 136.81, 138.29 (d, $^1J_{P-C}$ = 41.90 Hz, C-1), (phenyl group of P(CH$_3$)$_2$-Ph), 136.12, 136.48 (d, $^3J_{P-C}$ = 3 Hz, Nb=C=C), 366.55, 369.63 (broad, Nb=C=C). Anal. Calcd for C$_{32}$H$_{43}$BF$_4$NbPSi$_2$: C, 55.34; H, 6.24. Found: C, 53.99; H, 6.02.

Synthesis of [Nb($η^5$-C$_5$H$_4$SiMe$_3$)$_2$($η^2$(C,C)-HC≡CPh)-(CO)]$^+$ (5a). The synthesis of this cationic terminal alkyne complex was carried out through the facile conversion of the monovinylidene [Nb($η^5$-C$_5$H$_4$SiMe$_3$)$_2$(=C=CHPh)(CO)]$^+$ to the title complex, **5a**. Thus, a solution of [Nb($η^5$-C$_5$H$_4$SiMe$_3$)$_2$(=C=CHPh)(CO)][BPh$_4$] (**4a**[BPh$_4$]; 1:1 mixture of both *exo* and *endo* isomers (90 mg, 0.11 mmol)) in 5 mL of THF was stirred for 24 h at room temperature. After the solvent was removed in vacuo, an oily brown residue was obtained, which, after it was washed twice with diethyl ether, gave a pale brown solid identified as the *exo* isomer of [Nb($η^5$-C$_5$H$_4$SiMe$_3$)$_2$($η^2$(C,C)-HC≡CPh)(CO)][BPh$_4$] (85 mg, 0.10 mmol, 95%). Formation of the *endo* isomer was not observed. The product was recrystallized from a mixture of acetonitrile and diethyl ether to give pale yellow crystals. This reaction occurs readily at room temperature, in solvents such as THF and CD$_3$CN, to give the alkyne complex **5a**. The same reaction occurred when a solution of [Nb($η^5$-C$_5$H$_4$SiMe$_3$)$_2$(=C=CHPh)(CO)][BF$_4$] (**4a**[BF$_4$]) was stirred in THF. IR (KBr): $ν_{C≡C}$ 1772, $ν_{CO}$ 2044 cm^{-1}. ^{1}H NMR (CD$_3$CN): δ 0.03 (s, 18H, SiMe$_3$), 5.52−5.60 (2H), 5.62−5.72 (2H), 6.30−6.38 (2H), 6.46−6.56 (2H), (m, C$_5H_4$SiMe$_3$), 6.76−6.88 (m, 4H, p-C$_6$H$_5$), 6.92−7.04 (m, 8H, m-C$_6$H$_5$), 7.20−7.32 (m, 8H, o-C$_6$H$_5$) (phenyl groups of BPh$_4$$^-$), 7.38 (s, 1H, ≡CH), 7.40−7.60 (3H), 7.60−7.70 (2H) (m, C$_6H_5$ group of HC≡CC$_6$H$_5$). ^{13}C{^{1}H} NMR (CD$_3$CN): δ −1.13 (SiMe$_3$), 91.71, 103.06, 108.47, 108.76, 109.44 (C_5H_4SiMe$_3$), 111.51 (HC≡CC$_6$H$_5$), 122.73, 126.54, 136.69 (phenyl groups of BPh$_4$$^-$), 126.61, 130.02, 131.13, 133.63 (phenyl group of the ligand HC≡CC_6H_5), 132.08 (HC≡CC$_6$H$_5$), 164.74 (C$_{ipso}$ of phenyl groups of BPh$_4$$^-$, q, $J_{^{13}C-^{11}B}$ = 49 Hz). A signal corresponding to the CO carbon was not observed. Anal. Calcd for C$_{49}$H$_{52}$BNbOSi$_2$: C, 72.02; H, 6.37. Found: C, 71.95; H, 6.40.

Synthesis of [Nb($η^5$-C$_5$H$_4$SiMe$_3$)$_2$($η^2$(C,C)-HC≡C^{t}Bu)-(CO)]$^+$ (5c). A solution of [Nb($η^5$-C$_5$H$_4$SiMe$_3$)$_2$(=C=CH^{t}Bu)-

(CO)][BF$_4$] (**4c**[BF$_4$]; 40 mg, 0.07 mmol) in CD$_3$CN was placed in an NMR tube and left to stand at room temperature for 48 h. After this time the ^{1}H NMR spectrum showed two new compounds in a 1:1 ratio, which were identified as a mixture of both *endo* and *exo* isomers of the corresponding $η^2$-alkyne complex. Spectroscopic data for the mixture of the two new compounds are as follows. ^{1}H NMR (CD$_3$CN): *isomer I*, δ 0.18 (s, 18H, SiMe$_3$), 1.34 (s, 9H, ≡CCMe$_3$), 5.34−5.40 (2H), 5.94−6.00 (2H), 6.00−6.04 (2H), 6.18−6.24 (2H), (m, C$_5H_4$SiMe$_3$), 6.50 (s, 1H, C≡CH); *isomer II*, δ 0.31 (s, 18H, SiMe$_3$), 1.33 (s, 9H, ≡CCMe$_3$), 5.14−5.22 (2H), 5.28−5.34 (2H), 5.70−5.76 (2H), 6.24−6.30 (2H) (m, C$_5H_4$SiMe$_3$), 7.16 (s, 1H, C≡CH). ^{13}C{^{1}H} NMR (CD$_3$CN; mixture of both isomers): δ −0.32, −0.60 (SiMe$_3$), 30.79, 32.73 [C(CH_3)$_3$], 36.09, 38.40 [C(CH$_3$)$_3$], 84.32, 100.90, 103.21, 104.50, 104.87, 105.56, 108.79, 109.28, 111.91, 112.84 (C_5H_4SiMe$_3$), 127.48, 133.03, 144.56, 145.24 (HC≡C^tBu). The signal corresponding to CO is not observed. FAB MS (m/e (relative intensity)): 477 (94) (M$^+$, [Nb($η^5$-C$_5$H$_4$-SiMe$_3$)$_2$($η^2$(C,C)-HC≡C^{t}Bu)(CO)]$^+$), 449 (26) (M$^+$ − CO), 395 (100) (M$^+$ − HC≡C^{t}Bu), 367 (85) (M$^+$ − CO − HC≡C^{t}Bu).

Computational Details. Calculations were performed with the GAUSSIAN 94 series of programs[40] within the framework of the density functional theory (DFT)[41] using the B3LYP functional.[42] A quasi-relativistic effective core potential operator was used to represent the 28 innermost electrons of the niobium atom.[43] The basis set for the metal atom was that associated with the pseudopotential,[43] with a standard double-$ζ$ LANL2DZ contraction.[40] The 6-31G(d,p) basis set was used for the P, C$_α$, C$_β$, H$_α$, and Cl atoms and the carbonyl ligand, whereas the 6-31G basis set was used for the other carbon and hydrogen atoms.[44] To back up the methodology employed, vinylidene/alkyne systems that have been studied previously were reoptimized using the B3LYP functional and basis set of the same quality as used for the niobocene complexes: LANL2DZ basis set for metal atoms, 6-31G(d,p) basis set for the atoms directly attached to the metal and the acetylene and vinylidene ligands, and 6-31G basis set for the other atoms.[43,44] Our results for the RuCl$_2$(PH$_3$)$_2$ and RhCl-(PH$_3$)$_2$ systems (vinylidene isomer 13.7 and 6.3 kcal/mol more stable than the alkyne, respectively) are in reasonable agreement with those previously reported at the MP2 level (19.5[28a] and 7.8 kcal/mol,[28b] respectively). The higher stability of the $η^2$-alkyne isomer in F$_4$W (8.1 kcal/mol) also agrees with previous CCSD(T)//DFT calculations (10.4 kcal/mol).[28c] The calculated relative energy for the free vinylidene with respect to acetylene (41.8 kcal/mol) also reproduces previous theoretical[45] and experimental[46] results.

C_s symmetry has been maintained in the geometry optimizations. All stationary points were optimized with analytical

(40) Frisch, M. J.; Trucks, G. W.; Schlegel, H. B.; Gill, P. M. W.; Johnson, B. G.; Robb, M. A.; Cheeseman, J. R.; Keith, T. A.; Petersson, G. A.; Montgomery, J. A.; Raghavachari, K.; Al-Laham, M. A.; Zakrzewski, V. G.; Ortiz, J. V.; Foresman, J. B.; Cioslowski, J.; Stefanov, B. B.; Nanayakkara, A.; Challacombe, M.; Peng, C. Y.; Ayala, P. Y.; Chen, W.; Wong, M. W.; AndrJs, J. L.; Replogle, E. S.; Gomperts, R.; Martin, R. L.; Fox, D. J.; Binkley, J. S.; Defrees, D. J.; Baker, J.; Stewart, J. J. P.; Head-Gordon, M.; Gonzalez, C.; Pople, J. A. Gaussian 94; Gaussian Inc., Pittsburgh, PA, 1995.

(41) (a) Parr, R. G.; Yang, W. *Density Functional Theory of Atoms and Molecules*; Oxford University Press: Oxford, U.K., 1989. (b) Ziegler, T. *Chem. Rev.* **1991**, *91*, 651.

(42) (a) Lee, C.; Yang, W.; Parr, R. G. *Phys. Rev. B* **1988**, *37*, 785. (b) Becke, A. D. *J. Chem. Phys.* **1993**, *98*, 5648. (c) Stephens, P. J.; Devlin, F. J.; Chabalowski, C. F.; Frisch, M. J. *J. Phys. Chem.* **1994**, *98*, 11623.

(43) Hay, P. J.; Wadt, W. R. *J. Chem. Phys.* **1985**, *82*, 299.

(44) (a) Francl, M. M.; Pietro, W. J.; Hehre, W. J.; Binkley, J. S.; Gordon, M. S.; Defrees, D. J.; Pople, J. A. *J. Chem. Phys.* **1982**, *77*, 3654. (b) Hehre, W. J.; Ditchfield, R.; Pople, J. A. *J. Chem. Phys.* **1972**, *56*, 2257. (c) Hariharan, P. C.; Pople, J. A. *Theor. Chim. Acta* **1973**, *28*, 213.

(45) See for example: (a) Gallo, M. M.; Hamilton, T. P.; Schaefer, H. F. *J. Am. Chem. Soc.* **1990**, *112*, 8714. (b) Peterson, G. A.; Tensfeldt, T. G.; Montgomery, J. A., Jr. *J. Am. Chem. Soc.* **1992**, *114*, 6133. (c) Jensen, J. H.; Morokuma, K.; Gordon, M. S. *J. Chem. Phys.* **1994**, *100*, 1981.

first derivatives. Transition states were located by means of approximate Hessians and synchronous transit-guided quasi-Newtonian methods.[47] Most of the transition states located are similar to those already characterized in previous theoretical studies of the η^2-alkyne $\rightarrow \eta^1$-vinylidene isomerization. For this reason, and for computational limitations owing to the size of the systems considered, we have not fully characterized them. However, due to the differences between our transition state for the 1,3-hydrogen migration and published transition states for this mechanism, and also as an additional check, we did compute numerically the full Hessian for transition state **TS3n**[PH₃].

Atomic charges have been calculated, maintaining the NBO partitioning scheme.[48] Bader's topological analysis of the electron density[36] was performed using the XAIM 1.0 program.[49]

X-ray Data Collection for 5a. Crystals of **5a** were grown from a mixture of acetonitrile and diethyl ether. A suitable crystal was sealed in a Lindeman capillary tube under dry nitrogen and used for data collection. Reflections were collected at 25 °C on a NONIUS-MACH3 diffractometer equipped with a graphite-monochromated radiation source ($\lambda = 0.7107$ Å). Unit cell dimensions were obtained by a least-squares fit of the 2θ values of 25 high-order reflections by using the MACH3 centering routines. Crystal are monoclinic, space group $P2_1/c$, with $Z = 4$: $M_r = 816.81$, $a = 13.458(1)$ Å, $b = 13.544(9)$ Å, $c = 24.736(3)$ Å, $\beta = 94.51(1)°$. The intensities of 10 826 reflections were collected ($2 < \theta < 28°$); of these, only 3456

reflections obeyed the condition $I > 2\sigma(I)$. Data were corrected in the usual fashion for Lorentz and polarization effects, and a semiempirical absorption correction was applied.[50] The structure was solved by direct methods,[51] and refinement on F^2 was carried out by full-matrix least-squares analysis.[52] A number of cycles of refinement with isotropic thermal parameters, followed by difference synthesis, enabled location of all the non-hydrogen atoms. The SiMe₃ groups are disordered, and occupancies were refined initially and then fixed. Isotropic temperature parameters were considered for these atoms and anisotropic thermal parameters on the remaining atoms. The hydrogen atoms were included in calculation positions but were not refined. Weights were optimized in the final cycles. Refinement converged at the following reliability values: R1 = 0.0577 (for reflections with $I > 2\sigma(I)$), $S = 0.898$. Other detailed data are supplied in the Supporting Information.

Supporting Information Available: Tables of crystal data, structure solution and refinement details, atomic coordinates, bond lengths and angles, and anisotropic thermal parameters for $[Nb(\eta^5\text{-}C_5H_4SiMe_3)_2(\eta^2(C,C)\text{-HC}\equiv CPh)(CO)]\text{-}$ [BPh₄] (**5a**[BPh₄]). This material is available free of charge via the Internet at http://pubs.acs.org.

OM990957E

(46) (a) Ervin, K. M.; Ho, J.; Lineberger, W. C. *J. Chem. Phys.* **1989**, *91*, 5974. (b) Ervin, K. M.; Gronert, S.; Barlow, S. E.; Gilles, M. K.; Harrison, A. G.; Bierbaum, V. M.; De Puy, C. H.; Lineberger, W. C.; Ellison, G. B. *J. Am. Chem. Soc.* **1990**, *112*, 5750. (c) Chen, Y.; Jonas, D. M.; Hamilton, C. E.; Green, P. G.; Kinsey, J. L.; Field, R. W. *Ber. Bunsen-Ges. Phys. Chem.* **1988**, *92*, 329. (d) Chen, Y.; Jonas, D. M.; Kinsey, J. L.; Field, R. W. *J. Chem. Phys.* **1989**, 91, 3976.

(47) Peng, C.; Ayala, P. Y.; Schlegel, H. B.; Frisch, M. J. *J. Comput. Chem.* **1996**, *17*, 49.

(48) Reed, A. E.; Curtiss, L. A.; Weinhold, F. *Chem. Rev.* **1988**, *88*, 899.

(49) This program was developed by Jose Carlos Ortiz and Carles Bo, Universitat Rovira i Virgili, Tarragona, Spain.

(50) North, A. C. T.; Phillips, D. C.; Mathews, F. S. *Acta Crystallogr.* **1968**, *A24*, 351–359.

(51) Altomare, A.; Cascarano, G.; Giacovazzo, C.; Guagliardi, A.; Burla, M. C.; Polidori, G.; Camalli, M. *J. Appl. Crystallogr.* **1994**, 435–436.

(52) Sheldrick, G. M. *Program for the Refinement of Crystal Structures from Diffraction Data*; University of Göttingen, Göttingen, Germany, 1993.